

Analysis of site-response residuals from empirical ground-motion models to account for observed sedimentary basin effects in Wellington, New Zealand

Earthquake Spectra

2024, Vol. 40(4) 2475–2503

© The Author(s) 2024



Article reuse guidelines:

sagepub.com/journals-permissions

DOI: 10.1177/87552930241270562

journals.sagepub.com/home/eqs

Christopher A de la Torre, M.EERI¹, Brendon A Bradley, M.EERI¹, Robin L Lee, M.EERI¹, Ayushi Tiwari, M.EERI¹, Liam M Wotherspoon, M.EERI², Joel N Ridden¹, and Anna E Kaiser³

Abstract

Analysis of prediction–observation residuals from the empirical ground-motion models (GMMs) used in the 2022 New Zealand National Seismic Hazard Model (NZ NSHM) update indicates a general underprediction of ground motions in the period range of 0.5 – 2 s for soft sedimentary basin sites in Wellington. This study uses residual analysis to quantify this underprediction, understand the spatial distribution of these residuals and the specific conditions that cause them, and investigate options for the development of non-ergodic site-response adjustments to the GMMs. All 15 GMMs used in the NZ NSHM were evaluated, and the variability in site-response residuals between different models and different tectonic types of earthquake sources was quantified. Sites are regionalized based on different geomorphic features, such as individual basins and valleys. For example, average site terms are calculated for Te Aro, Thorndon, Miramar, Lower Hutt, Upper Hutt, and several smaller valleys. The period at which maximum underprediction occurs at these sedimentary basin and valley sites was found to correlate well with the fundamental site period of the soil profile (T_0), suggesting improvements can be made to regionalized GMMs by incorporating site period into the site-response prediction for sedimentary basin sites.

¹Department of Civil and Natural Resources Engineering, University of Canterbury, Christchurch, New Zealand

²Department of Civil and Environmental Engineering, University of Auckland, Auckland, New Zealand

³GNS Science, Lower Hutt, New Zealand

Corresponding author:

Christopher A de la Torre, Department of Civil and Natural Resources Engineering, University of Canterbury, Private Bag 4800, Christchurch 8140, New Zealand.

Email: christopher.delatorre@canterbury.ac.nz

Keywords

Site effects, basin effects, residual analysis, ground-motion modeling, Wellington basin, non-ergodic site response

Date received: 17 December 2023; accepted: 10 June 2024

Introduction

Historically, empirical ground-motion models (GMMs) have utilized the ergodic assumption (Anderson and Brune, 1999) to predict the mean and standard deviation of earthquake ground-motion amplitudes for sites within broad tectonic categories. Combining ground-motion observations from similar tectonic regions around the world produces sufficient data to constrain global models that are, on average, unbiased. However, because of region-specific variations in earthquake source characteristics, path attenuation, and geologic/geomorphic site conditions, these ergodic global models have large aleatory variabilities (Kotha et al., 2016; Lavrentiadis et al., 2023) and can be biased for specific regions. Bias and variability can also arise from limitations on the data used to constrain these models, for example, the sparsity of soft-soil sites in ground-motion databases (e.g., Campbell and Bozorgnia, 2014).

The comparison of residual standard deviations between global models and site-specific applications illustrates a reduction in variability when site response is constrained at a site using residual analysis from observations (Atkinson, 2006; Lin et al., 2011; Rodriguez-Marek et al., 2011). This reduction in standard deviation, or total sigma, can be on the order of 10%–15% and can be increased to approximately 40% when single-path effects are considered for a given source region and site combination. Efforts continue to further reduce the extent to which the ergodic assumption is employed in empirical GMMs by creating region- or site-specific models.

These models range from regional-scale models that include non-ergodic components for the source, path, and site (Abrahamson et al., 2019; Landwehr et al., 2016; Macedo and Liu, 2022; Sung et al., 2023; Villani and Abrahamson, 2015), to site-specific and basin-specific models that focus on non-ergodic site effects (Rodriguez-Marek et al., 2014; Sung and Abrahamson, 2022). For example, Parker and Baltay (2022) and Nweke et al. (2022) used earthquake observations in the Los Angeles sedimentary basin to empirically constrain site response in the area, while Sung and Abrahamson (2022) used 3D simulations of the Cascadia subduction zone to adjust the Abrahamson and Gülerce (2020) GMM to account for amplification of the Seattle basin. In NZ, Bradley (2013) modified the Chiou and Youngs (2014) GMM based on a NZ-specific crustal earthquake data set, and Bradley (2015) developed non-ergodic adjustment factors for application of this GMM to the Canterbury region. These models sit on an ergodic continuum (e.g., Chapter 8 in Baker et al., 2021) that ranges between the extremes of ergodic, and fully non-ergodic, and is governed by the extent of region- and site-specific data used to constrain the model.

The NGA-West2 (Bozorgnia et al., 2014) and NGA-Sub (Bozorgnia et al., 2022) projects were global efforts to improve GMMs for crustal and subduction regions, respectively. The GMMs developed, which are commonly used in nationwide and site-specific probabilistic seismic hazard analyses (Gerstenberger et al., 2024; Petersen et al., 2020), include global versions and regionalizations for broad geographic regions. For example, the Kuehn et al. (2020), Abrahamson and Gülerce (2020), and Parker et al. (2022)

GMMs have regionalization for Japan, Cascadia, Taiwan, Alaska, and other regions around the world. The Next Generation Attenuation (NGA)-West2 and NGA-Sub GMMs were used in the 2022 New Zealand National Seismic Hazard Model (NZ NSHM) update (Bradley et al., 2024). Although some of the NGA-Sub models include NZ-specific regionalizations, these models encompass NZ as a whole, not individual basins such as the Wellington basin. In addition, these NZ-specific regionalizations are constrained with a sparse data set, particularly for the magnitude and distance bins that dominate the hazard (Bradley et al., 2024). These sentiments highlight that additional work is required to regionalize models to account for small-scale basin-specific site amplification globally, and in a New Zealand context.

The Wellington basin, in the capital city of NZ, has been observed to strongly amplify ground motions, especially in the vibration period range of $T=0.5 - 2$ s (Adams et al., 2012; Bradley et al., 2018; de la Torre et al., 2024; Kaiser et al., 2020). Studies from the 2022 NZ NSHM have demonstrated that empirical GMMs generally underpredict the observed site amplification in Wellington due to combined basin and site effects for soft sedimentary basin sites (de la Torre et al., 2024; Kaiser et al., 2022). Wellington has a high seismic hazard as it is underlain by the Wellington and Aotea faults, and is in close proximity to the Hikurangi subduction zone, making it critical to understand patterns of site amplification and the performance of GMMs in this region.

This article focuses on quantifying the performance of empirical GMMs at predicting site-specific ground motions in the Wellington region of New Zealand. It is the first study that rigorously and systematically assesses residuals in the Wellington region. Unlike prior non-ergodic site-response studies that have considered a single GMM (e.g., Atkinson, 2006; Bradley, 2015; Rodriguez-Marek et al., 2011; Sung and Abrahamson, 2022), this study evaluates all 15 GMMs used in the NZ NSHM logic tree for developing site and basin-specific regionalizations of site-response residuals for all the GMMs. Models from different tectonic types are compared, and the variability between these models is assessed. Site terms are grouped geographically by specific basin or valley sub-regions in Wellington to understand small-scale fluctuations in basin and site effects.

Ground motions and sites considered

Ground-motion database

We considered the data set of Lee et al. (2023), which is based on a subset of the New Zealand ground-motion database (NZ GMDB) v1.0 (Hutchinson et al., 2022). The remaining data set, after application of the filtering criteria imposed by Lee et al. (2023), contains 17,081 ground motions across New Zealand, of which 4,691 records exist at sites in the Wellington Region, including the Lower Hutt and Upper Hutt valleys. The filtering criteria by Lee et al. (2023) include minimum magnitude (3.5 and 4.5 for crustal and subduction, respectively), maximum rupture distance (300 and 500 km for crustal and subduction, respectively), accelerometer channels only, and a minimum usable frequency. In addition, we impose a minimum number of three records per event and site for each intensity measure (IM) to robustly calculate event and site residuals. Figure 1 shows the distributions of M_W and R_{rup} for the NZ-wide data set and the Wellington region subset. The Wellington subset of ground motions are colored by tectonic type of the event corresponding to each ground motion, showing that the database has significantly more shallow crustal than subduction interface or slab ground-motion records. As tabulated in the top right

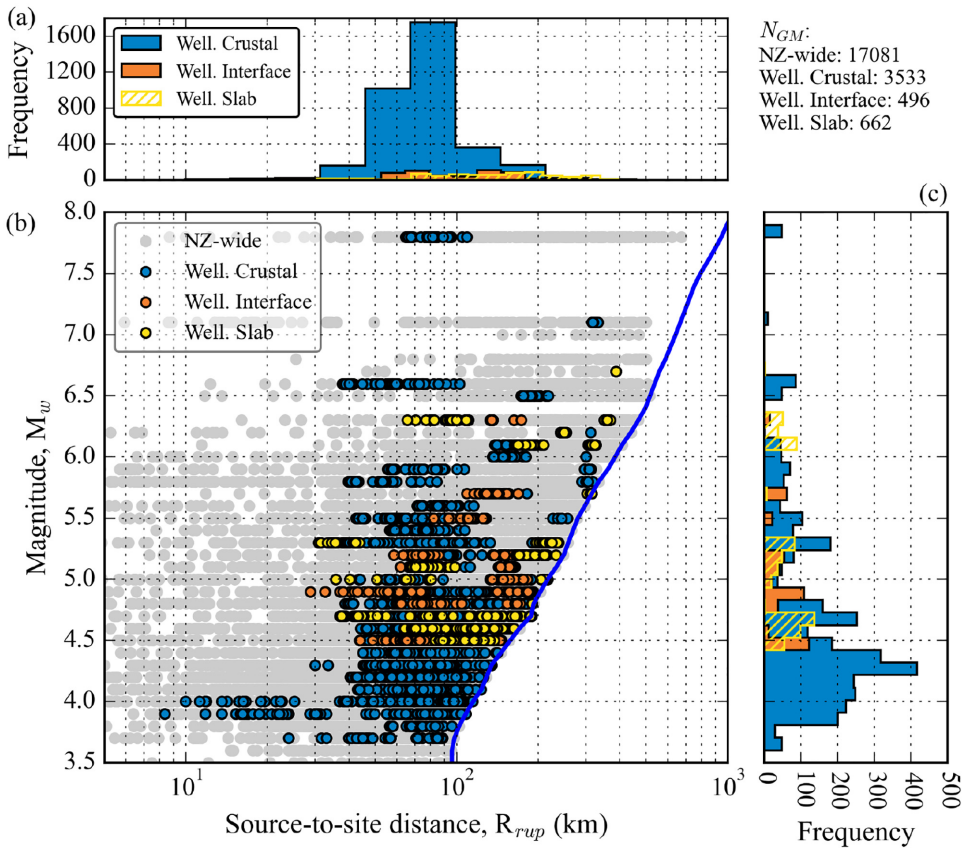


Figure 1. Earthquake source and ground-motion M_w and R_{rup} distributions for the NZ-wide and Wellington ground-motion data sets. The subset of ground motions recorded at Wellington strong motion stations (SMSs) are color-coded by tectonic type of the event as follows: blue for crustal, orange for interface, and yellow for slab. The gray markers represent the entire NZ-wide database for which the mixed-effects regression was performed to calculate partitioned residuals. The sub-figures are as follows: (a) source-to-site distance (R_{rup}) histogram; (b) magnitude versus source-to-site distance scatter plot; and (c) magnitude histogram (frequency counted by record). The blue line shows the M_w -dependent R_{rup} filter used by Lee et al. (2023).

corner of Figure 1, the Wellington region subset contains 3533 crustal, 496 interface, and 662 slab ground-motion records.

The spatial distribution of earthquake epicenters for the NZ-wide and Wellington region subsets of ground motions is shown in Figure 2 for crustal, and slab and interface subduction sources. The majority of crustal events recorded at Wellington SMSs are located around the north-east corner of the South Island, which could result in some mapping of path effects into the site residuals if the path effects of crustal events originating from the South Island and Cook Strait are not well captured. However, with inclusion of all tectonic types, there is generally good azimuthal coverage. In subsequent results, we show that site residuals are relatively consistent between tectonic type, illustrating that mapping of path effects to site terms is a second-order effect in this data set.

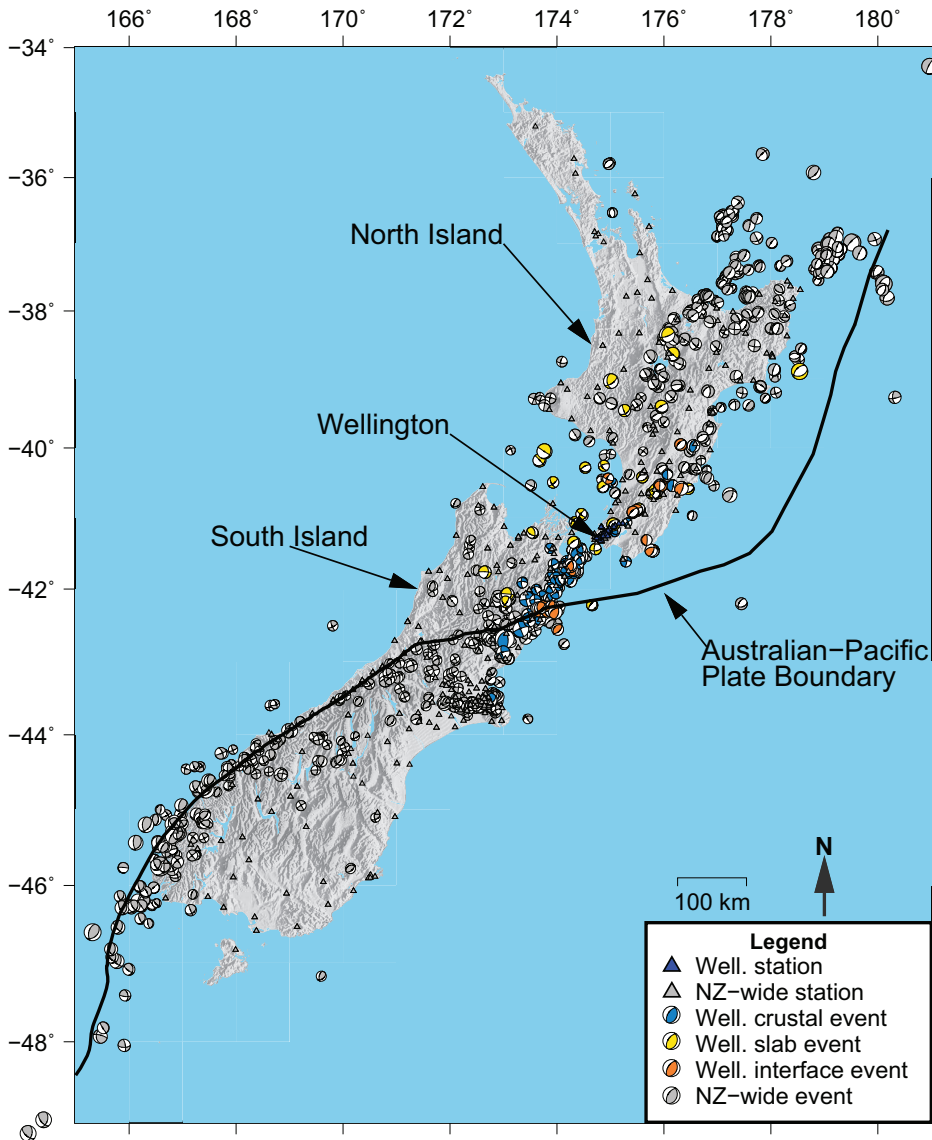


Figure 2. A map showing the spatial distribution of stations and earthquake epicenters used in this study. The colors in the legend distinguish between the Wellington region (“Well” in legend) subset of ground motions, and the NZ-wide subset for which the residual analysis was performed. Focal mechanisms for events with ground motions recorded at Wellington stations are color-coded based on event tectonic type. The size of all focal mechanisms is scaled by moment magnitude. The location of SMS in the Wellington region is shown in blue triangles.

Sites in the Wellington region

SMS sites in the greater Wellington region, including the surrounding hills and valleys, were subdivided based on location, geomorphic categorization, basin geometry, and site-response characteristics. The sub-regions considered generally correspond to specific sedimentary basins and valleys. These sub-regions include Te Aro, Thorndon, Lower Hutt,

Upper Hutt, Miramar, Karori, Porirua, and Wainuiomata, as identified on the map in Figure 3. Figure 4 provides more zoomed-in versions of Figure 3 for different regions and identifies the station IDs for all SMS. The Wellington Central Business District (CBD) spans across the Te Aro and Thorndon areas. Sites were also divided into four geomorphic categories including basin, basin edge, valley, and hill by Tiwari et al. (2023) using category definitions by Nweke et al. (2022). Table 1 provides metadata and site characteristics for all the sites in the greater Wellington region, including the depth to a shear wave velocity (V_S) of 1000 m/s ($Z_{1,0}$) and the time-averaged V_S in the upper 30 m (V_{S30}). The site metrics provided are based on the NZ site database by Wotherspoon et al. (2023). Importantly, some of these site parameters are classified as Q3 (i.e., the lowest quality ranking) in the database. These parameters are identified with a “*” in Table 1. A Q3 designation suggests that the parameter was inferred from regional-scale maps or is poorly constrained by data, and is not a site-specific measurement. While many of the basin sites analyzed in this study have Q1 or Q2 site parameters, this variable quality of site input parameters could contribute to the bias and variability observed in the residual analysis.

Methodology

Residual analysis

The performance of GMMs on a region-by-region and site-by-site basis is assessed using mixed-effects residual analysis to decompose the residual into its various components (e.g., Al Atik et al., 2010; Bradley, 2015). The total prediction residual, Δ_{es} , for spectral acceleration at a given oscillator period, T , can be expressed as:

$$\Delta_{es} = \ln SA_{es}^{Obs} - \ln SA_{es}^{GMM} \quad (1)$$

where $\ln SA_{es}^{Obs}$ is the natural logarithm of the observed spectral acceleration at an oscillator period T , for earthquake e at site s ; $\ln SA_{es}^{GMM}$ is the natural logarithm of the respective spectral acceleration predicted by a GMM. The IMs considered in this study are 5%-damped RotD50 response spectral accelerations (Boore, 2010) at 30 vibration periods between 0.01 and 10 s.

To identify systematic trends in prediction bias for a given GMM m , earthquake e , and site s , the prediction residual in Equation 1 is partitioned as:

$$\Delta_{es}^m = a^m + \delta B_e^m + \delta S2S_s^m + \delta W_{es}^{0,m} \quad (2)$$

where for each IM, a is a constant representing overall model bias for all earthquakes and sites considered, δB_e is the between-event residual for earthquake e , $\delta S2S_s$ is the site-to-site residual for site s , and δW_{es}^0 is the “remaining” within-event residual for earthquake e at site s . δB_e , $\delta S2S_s$, and δW_{es}^0 residuals are assumed to be normally distributed with zero mean and variances of τ^2 , ϕ_{S2S}^2 , and ϕ_{SS}^2 , respectively. Treating all terms as independent, the total variance, σ_T^2 , for model m , is then expressed as:

$$(\sigma_T^m)^2 = (\tau^m)^2 + (\phi_{S2S}^m)^2 + (\phi_{SS}^m)^2 \quad (3)$$

Table 1. Metadata for Wellington region strong motion stations (SMS)

| SMS ID | Latitude | Longitude | Region | Geomorphic category | Z _{1.0} (m) | T ₀ (s) | V ₃₃₀ (m/s) | NGM, s |
|--------|-----------|-----------|--------------------|---------------------|----------------------|--------------------|------------------------|--------|
| LHES | -41.21169 | 174.90334 | Lower Hutt | Basin | 175 | 1.16 ^a | 222 ^a | 66 |
| LHUS | -41.23085 | 174.89364 | Lower Hutt | Basin | 243 | 1.75 | 212 | 35 |
| LNBS | -41.20498 | 174.92660 | Lower Hutt | Basin | 131 | 0.80 ^a | 330 | 72 |
| LRSS | -41.22943 | 174.90425 | Lower Hutt | Basin | 200 | 1.72 | 256 | 39 |
| PGMS | -41.22451 | 174.87944 | Lower Hutt | Basin | 274 | 1.788 | 200 | 40 |
| PVCS | -41.22475 | 174.87392 | Lower Hutt | Basin | 296 | 2.0 | 190 | 29 |
| SEVS | -41.24698 | 174.90216 | Lower Hutt | Basin | 246 | 1.2 | 209 ^a | 31 |
| SOCS | -41.20433 | 174.91594 | Lower Hutt | Basin | 151 | 1.35 | 233 ^a | 72 |
| TAIS | -41.18038 | 174.95477 | Lower Hutt | Basin | 42 | 0.69 | 510 | 136 |
| DAVS | -41.20579 | 174.95436 | Lower Hutt | Basin edge | 35 ^a | 0.6289 | 300 ^a | 81 |
| LIRS | -41.23231 | 174.91929 | Lower Hutt | Basin edge | 16 | 0.25 | 400 ^a | 95 |
| NBSS | -41.20227 | 174.95376 | Lower Hutt | Basin edge | 47 | 0.9 | 190 | 61 |
| BMTS | -41.19137 | 174.92603 | Lower Hutt Hills | Hill | 15 ^a | 0.05 | 1000 ^a | 134 |
| FAIS | -41.20740 | 174.94010 | Lower Hutt Hills | Hill | 15 ^a | 0.05 | 1000 ^a | 180 |
| HSSS | -41.15194 | 174.98148 | Lower Hutt Hills | Hill | 9 | 0.22 | 526 ^a | 60 |
| INSS | -41.23352 | 174.92112 | Lower Hutt Hills | Hill | 28 ^a | 0.09 | 630 ^a | 46 |
| LHBS | -41.19665 | 174.89232 | Lower Hutt Hills | Hill | 23 ^a | 0.05 | 626 ^a | 115 |
| LHRS | -41.20474 | 174.89319 | Lower Hutt Hills | Hill | 0 | 0.05 | 622 ^a | 131 |
| PHFS | -41.25265 | 174.90455 | Lower Hutt Hills | Hill | 23 [*] | 0.05 [*] | 615 [*] | 10 |
| PHHS | -41.25209 | 174.90430 | Lower Hutt Hills | Hill | 23 ^a | 0.05 ^a | 613 ^a | 122 |
| PTOS | -41.22297 | 174.86030 | Lower Hutt Hills | Hill | 23 ^a | 0.20 ^a | 450 ^a | 138 |
| SOMS | -41.25746 | 174.86500 | Lower Hutt Hills | Hill | 15 ^a | 0.05 | 1000 ^a | 194 |
| WANS | -41.23121 | 174.93102 | Lower Hutt Hills | Hill | 15 ^a | 0.05 | 1000 ^a | 101 |
| MISS | -41.31489 | 174.81843 | Miramar and Karori | Valley | 97 | 1.15 | 274 | 45 |
| WNAS | -41.32641 | 174.80903 | Miramar and Karori | Valley | 66 | 1.12 | 229 | 51 |
| WNKS | -41.28482 | 174.74205 | Miramar and Karori | Valley | 39 | 0.31 | 369 | 143 |
| PFAS | -41.13849 | 174.84610 | Porirua | Valley | 0 | 0.11 | 532 ^a | 109 |
| POKS | -41.12495 | 174.83151 | Porirua | Valley | 33 ^a | 0.28 | 302 ^a | 130 |
| POLS | -41.13139 | 174.83910 | Porirua | Valley | 25 | 0.4 | 275 ^a | 89 |
| PWES | -41.12746 | 174.82586 | Porirua Hills | Hill | 25 ^a | 0.05 | 622 ^a | 160 |
| CUBS | -41.29546 | 174.77438 | Te Aro | Basin | 47 | 0.63 | 339 ^a | 19 |

(continued)

Table 1. Continued

| SMS ID | Latitude | Longitude | Region | Geomorphic category | Z _{1.0} (m) | T ₀ (s) | V ₅₃₀ (m/s) | N _{GM_s} |
|--------|-----------|-----------|------------------|---------------------|----------------------|--------------------|------------------------|-----------------------------|
| TEPS | -41.29059 | 174.78106 | Te Aro | Basin | 103 | 0.99 | 292 | 55 |
| FKPS | -41.28795 | 174.77876 | Te Aro | Basin edge | 30 | 0.41 | 323 | 85 |
| RQGS | -41.29653 | 174.78115 | Te Aro | Basin | 46 | 0.6 | 246 | 16 |
| TRTS | -41.29870 | 174.77390 | Te Aro | Basin edge | 29 | 0.28 | 400 | 99 |
| WCFS | -41.29315 | 174.78479 | Te Aro | Basin edge | 7 | 0.24 | 589 | 13 |
| WTYS | -41.29543 | 174.78126 | Te Aro | Basin | 49 | 0.8 | 230 ^a | 14 |
| CPLB | -41.27881 | 174.78209 | Thorndon | Basin | 247 | 1.21 | 244 | 142 |
| PIPS | -41.26749 | 174.78607 | Thorndon | Basin | 157 | 1.0 | 210 | 23 |
| TFSS | -41.27543 | 174.78305 | Thorndon | Basin | 157 | 1.73 | 271 | 87 |
| WEMS | -41.27429 | 174.77926 | Thorndon | Basin | 128 | 0.98 | 312 | 80 |
| BOWS | -41.27919 | 174.77632 | Thorndon | Basin edge | 65 | 0.62 | 325 | 78 |
| VUWS | -41.27985 | 174.77840 | Thorndon | Basin edge | 70 | 0.87 | 286 | 120 |
| HIBS | -41.13990 | 175.03590 | Upper Hutt | Basin | 103 ^a | 1.0 | 500 ^a | 74 |
| UHCS | -41.12681 | 175.04094 | Upper Hutt | Basin | 136 | 2.0 | 390 | 87 |
| UHSS | -41.12638 | 175.06509 | Upper Hutt | Basin | 104 | 0.9 | 481 | 125 |
| TOTS | -41.10492 | 175.08539 | Upper Hutt | Basin edge | 22 | 1.00 ^a | 500 ^a | 79 |
| KIRS | -41.07688 | 175.23001 | Upper Hutt Hills | Hill | 43 ^a | 0.43 | 329 ^a | 105 |
| TMDS | -41.07808 | 175.15544 | Upper Hutt Hills | Hill | 10 ^a | 0.05 ^a | 800 ^a | 69 |
| ARKS | -41.24208 | 174.94410 | Wainuiomata | Valley | 20 | 0.37 | 267 ^a | 171 |
| PRKS | -41.24902 | 174.93413 | Wainuiomata | Valley | 70 | 0.8 | 190 | 30 |
| WDAS | -41.25740 | 174.94847 | Wainuiomata | Valley | 62 | 1.25 | 120 | 21 |
| SEAS | -41.32645 | 174.83764 | Wellington Hills | Hill | 53 ^a | 0.3 | 305 | 92 |
| POTS | -41.27222 | 174.77464 | Wellington Hills | Hill | 24 | 0.24 | 453 | 67 |
| WEL | -41.28405 | 174.76818 | Wellington Hills | Hill | 0 | 0.05 ^a | 687 ^a | 155 |
| WNHS | -41.30078 | 174.77551 | Wellington Hills | Hill | 50 | 0.32 | 493 | 69 |
| WTES | -41.28158 | 174.77419 | Wellington Hills | Hill | 7 | 0.09 | 334 ^a | 16 |

N_{GM_s}: total number of ground motions used for site s.

^aThe site parameter is listed as Q3 (the lowest quality) in the site database (Wotherspoon et al., 2023), meaning that the values are either inferred from regional-scale maps or poorly constrained, and not site-specific measurements.

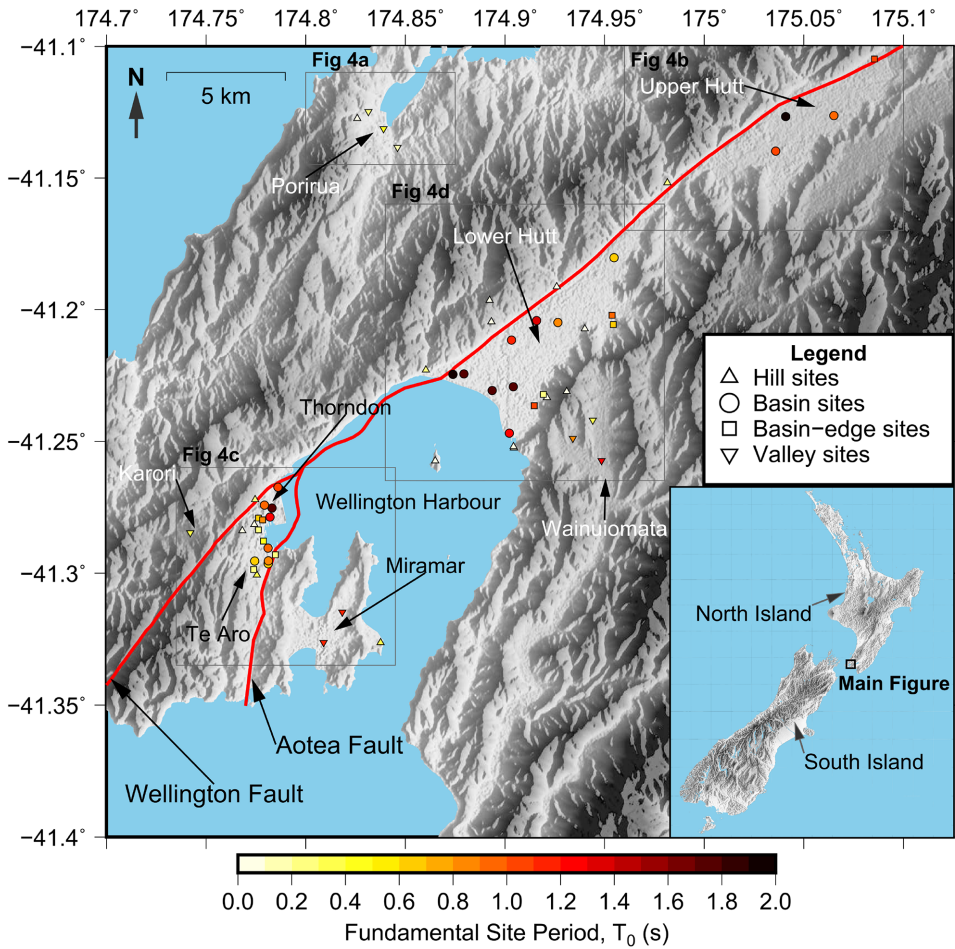


Figure 3. A map showing the location of all sites in the greater Wellington region. Site symbols are color-coded by T_0 and the symbol shape indicates the geomorphic category assigned to each site as indicated in the legend. Zoomed-in versions with SMS labels are shown in Figure 4.

GMMs investigated and weighting scheme

All 15 GMMs used in the 2022 NZ NSHM (Bradley et al., 2024) are included in the subsequent analysis. In addition to model-specific mixed-effects residuals, we also sought to compute a resulting weighted average over all GMMs considered. The model-specific weight (w_T^m) is comprised of two parts:

$$w_T^m = w_{NSHM}^m \times w_{Ngm}^m \quad (4)$$

where w_{NSHM}^m was the weight given to the model in the NSHM logic tree (see Table 2; Bradley et al., 2024; Gerstenberger et al., 2024) and w_{Ngm}^m is a function of the number of ground motions that were used in the mixed-effects residual analysis for each tectonic type. Specifically, this was done because there are nearly 10 times more crustal events than subduction events in the data set; therefore, it is logical that the resulting residuals are

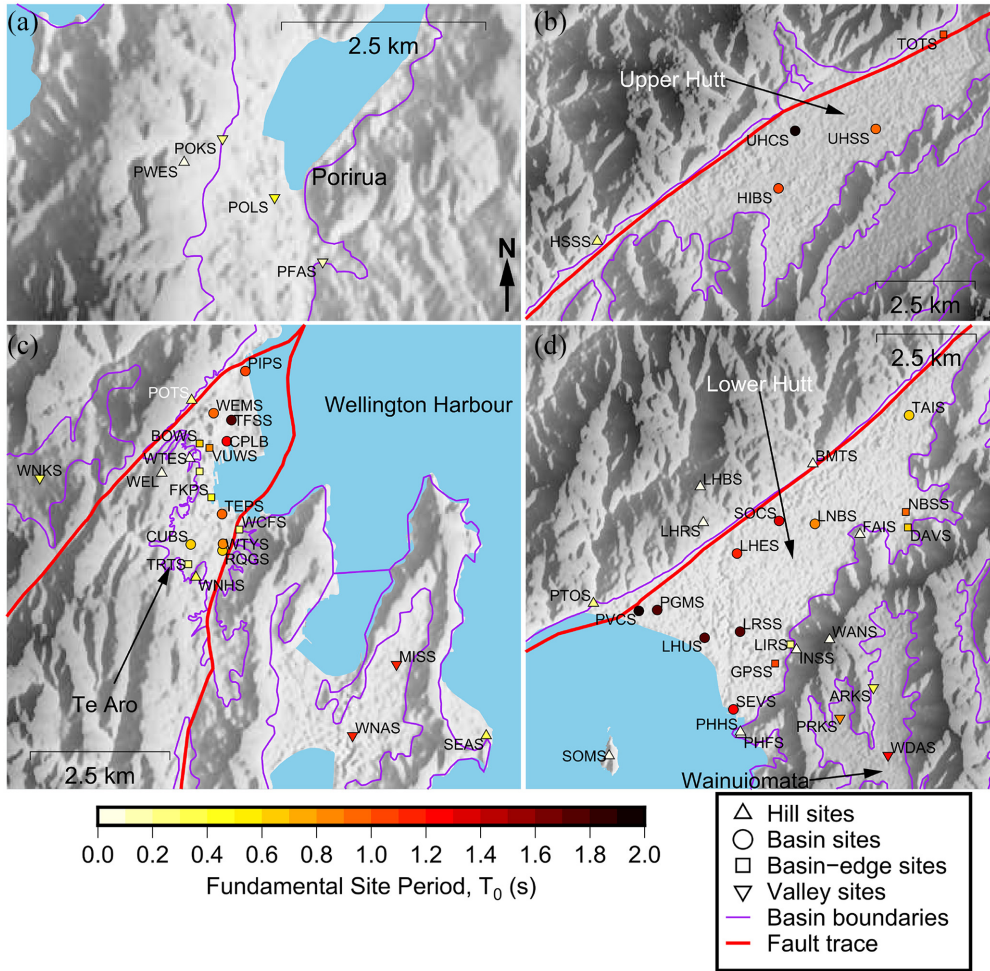


Figure 4. Maps identifying the station ID for all SMS considered in the Wellington region divided into regions as (a) Porirua, (b) Upper Hutt, (c) Wellington CBD, Karori, and Miramar, and (d) Lower Hutt and Wainuiomata. The locations of each subfigure, relative to the entire Wellington region, are identified in Figure 3. Site symbols are color-coded by T_0 and the symbol shape indicates the geomorphic category assigned to each site as indicated in the legend.

more statistically stable. Hence, $w_{N_{gm}}^m$ was assigned in proportion to the error in the sample mean, which scales as $1/\sqrt{N}$. For example, crustal models had a weighting of:

$$w_{N_{gm},crustal}^m = \frac{\sqrt{N_{GM,crustal}}}{\sqrt{N_{GM,crustal} + \sqrt{N_{GM,slab}} + \sqrt{N_{GM,interface}}}} \quad (5)$$

where $(N_{GM,crustal}, N_{GM,slab}, N_{GM,interface}) = (3538, 506, 666)$ as previously discussed with reference to Figure 1. Table 2 lists the considered models, their tectonic type, and respective weights. A detailed description of the models in the context of the NZ NSHM is given by Bradley et al. (2024).

Table 2. Empirical GMMs and weights used in this study based on the NZ NSHM.

| Model ID | Reference | Tectonic type and weight, w_{Ngm}^m | NSHM weight, w_{NSHM}^m | Total weight, w_T^m |
|----------|-------------------------------|---------------------------------------|---------------------------|-----------------------|
| A22 | Atkinson (2022) | Crustal: 0.552 | 0.28 | 0.15456 |
| S22 | Stafford (2022) | | 0.39 | 0.21528 |
| ASK14 | Abrahamson et al. (2014) | | 0.066 | 0.036432 |
| CY14 | Chiou and Youngs (2014) | | 0.066 | 0.036432 |
| CB14 | Campbell and Bozorgnia (2014) | | 0.066 | 0.036432 |
| BSSA14 | Boore et al. (2014) | | 0.066 | 0.036432 |
| Br13 | Bradley (2013) | | 0.066 | 0.036432 |
| A22 | Atkinson (2022) | Interface: 0.209 | 0.27 | 0.05643 |
| AG20 | Abrahamson and Gülerce (2020) | | 0.25 | 0.05225 |
| K20 | Kuehn et al. (2020) | | 0.24 | 0.05016 |
| P21 | Parker et al. (2022) | | 0.24 | 0.05016 |
| A22 | Atkinson (2022) | Slab: 0.239 | 0.28 | 0.06692 |
| AG20 | Abrahamson and Gülerce (2020) | | 0.25 | 0.05975 |
| K20 | Kuehn et al. (2020) | | 0.24 | 0.05736 |
| P21 | Parker et al. (2022) | | 0.23 | 0.05497 |

Computation of the weighted mean, $\overline{\delta S2S}_s$, and between-model variability, $\sigma_{\delta S2S,s}^{B-m}$

As described in the ‘‘Residual analysis’’ section, the site-to-site residual is calculated for every site s and GMM m and is denoted as $\delta S2S_s^m$. The weighted mean of $\delta S2S_s^m$, for all GMMs at a given site, s , is calculated as:

$$\overline{\delta S2S}_s = \sum_{m=1}^{N_{GMMs}} \delta S2S_s^m \times w_T^m \quad (6)$$

where w_T^m are the total weights for each GMM given in Table 2, and $N_{GMM} = 15$ is the number of GMMs considered. To quantify the variation in $\delta S2S$ values computed from the different GMMs, we compute a between-model standard deviation, $\sigma_{\delta S2S,s}^{B-m}$, as the weighted standard deviation of all the site terms from all the GMMs at a given site s , specifically:

$$\sigma_{\delta S2S,s}^{B-m} = \sqrt{\sum_{m=1}^{N_{GMMs}} w_T^m \times (\delta S2S_s^m - \overline{\delta S2S}_s)^2} \quad (7)$$

We subsequently also consider the mean and standard deviation of $\overline{\delta S2S}_s$ for all sites in a particular region R (e.g., the basin sub-regions of Thorndon, Te Aro, and Lower Hutt), which are expressed as:

$$\overline{\delta S2S}_R = \frac{1}{N_{sites}} \sum_{s=1}^{N_{sites}} \overline{\delta S2S}_s \quad (8)$$

$$\phi_{S2S,R} = \sqrt{\frac{1}{N_{sites} - 1} \sum_{s=1}^{N_{sites}} (\overline{\delta S2S}_s - \overline{\delta S2S}_R)^2} \quad (9)$$

where N_{sites} is the number of sites within the region. Finally, the average between-model standard deviation across all sites in a region is defined as:

$$\overline{\sigma}_{\delta S2S_s, R}^{B-m} = \frac{1}{N_{sites}} \sum_{s=1}^{N_{sites}} \sigma_{S2S_s, s}^{B-m} \quad (10)$$

Residual analysis results

Between-model variability in site-specific residuals

Figure 5 illustrates the site-to-site residuals, $\delta S2S_s^m$, and the systematic site term, $a^m + \delta S2S_s^m$, for all GMMs at two example basin sites in the Wellington CBD. For both sites, all GMMs underpredict (positive residuals) in the period range corresponding to basin amplification in the Wellington basin (i.e., $T = 0.5 - 2$ s) and is most pronounced around the experimentally measured fundamental site period, T_0 .

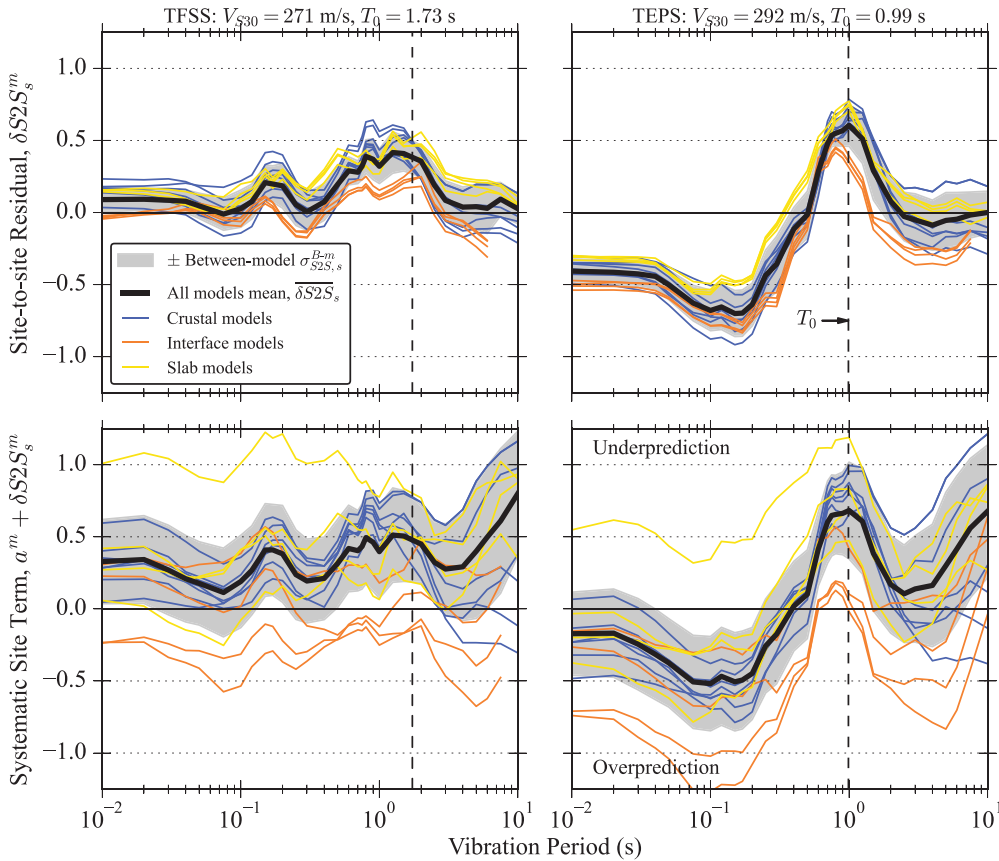


Figure 5. Site-to-site residuals, $\delta S2S_s^m$ (top panels), and systematic site terms, $a^m + \delta S2S_s^m$ (bottom panels), as a function of period for two example basin sites in the Wellington region. For each site, $\delta S2S_s^m$ from individual GMMs are included as well as the weighted mean ($\delta S2S_s$) and standard deviation ($\sigma_{S2S_s}^{B-m}$) of all GMMs from Equations 6 and 7. Lines for individual GMMs are color-coded by tectonic type (i.e., crustal, interface, and slab).

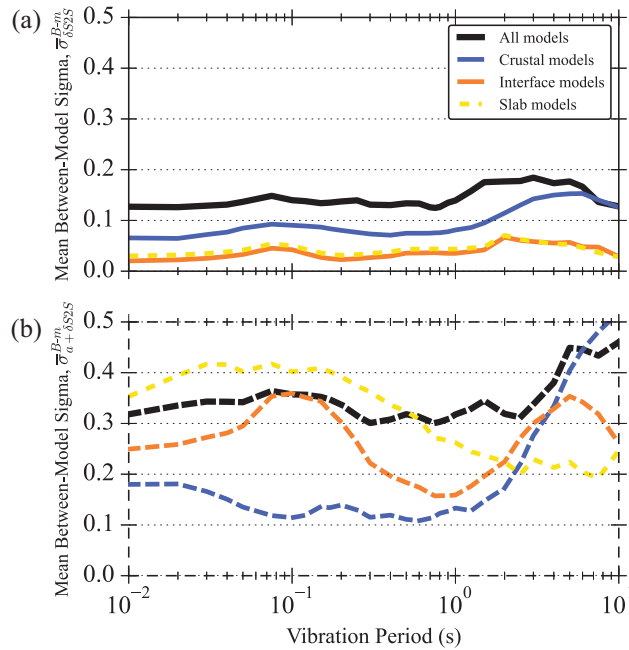


Figure 6. Mean between-model standard deviations of (a) $\delta S2S_s^m$ and (b) $a^m + \delta S2S_s^m$ for crustal, interface, slab, and all models for all sites in the Wellington region.

It is apparent from Figure 5 that the between-model variability is significantly lower for $\delta S2S_s^m$ than for $a^m + \delta S2S_s^m$ for both sites. Considering that $\delta S2S_s^m$ represents repeatable site effects at site s , whereas $a^m + \delta S2S_s^m$ represents repeatable source, path, and site effects at site s ; this illustrates that the variability in unexplained site response between the GMMs is relatively low compared with the unexplained source and path effects. This is likely because several of the GMMs use similar formulations for the site response, thus yielding similar site-response predictions. The variability in the overall model bias is higher (bottom panels of Figure 5), implying that there are greater differences between GMMs in components other than the site-response models (e.g., more complicated path and source effects). This point is highlighted again in Figure 6, which shows that the average of $\sigma_{\delta S2S_s^m}^{B-m}$ across all sites in the Wellington region ($\bar{\sigma}_{\delta S2S_s^m}^{B-m}$; Equation 10) is approximately 0.12 – 0.19 in natural log units compared with the average between-model variability in $a^m + \delta S2S_s^m$ that ranges from 0.3 – 0.45 in natural log units. Figure 6 also shows that $\bar{\sigma}_{\delta S2S_s^m}^{B-m}$ is even lower between models of the same tectonic type. When the variability in bias is also included (i.e., Figure 6b) the subduction GMMs have significantly higher variability between models for $T < 1$ s. However, for $T > 1$ s, different crustal GMMs use fundamentally different approaches for how they constrain the long-period amplitudes, resulting in a large increase in $\bar{\sigma}_{a^m + \delta S2S_s^m}^{B-m}$ for these crustal GMMs. For further discussion on the total bias for individual GMMs, the reader is referred to Lee et al. (2023).

Interestingly, the site terms between interface and slab events are different even though the predictions for these subduction ground motions use the same base GMMs (refer to Table 2). For example, in Figure 5, the peak value of the site terms for interface events is approximately 50% lower than that from slab and crustal events. Figure A.1 in the Online Supplemental Material, which plots site terms for all sites in three of the basin sub-region

separated by tectonic type, also shows that the interface models produce lower peak values of the site term than slab and crustal models across the board. This illustrates, in our opinion, that source and path effects are being mapped into the systematic site term. This is one reason why some previous studies include an additional path-to-path term in the regression and consider single-path effects (e.g., Al Atik et al., 2010; Lin et al., 2011; Rodriguez-Marek et al., 2011).

Previous studies focusing on the removal of the ergodic assumption in site-response models of GMMs have generally focused on a single GMM (e.g., Atkinson, 2006; Bradley, 2015; Rodriguez-Marek et al., 2011; Sung and Abrahamson, 2022); however, in probabilistic seismic hazard analysis (PSHA) applications, a logic tree containing many GMMs is required (Chapter 6 in Baker et al., 2021). One of the novelties of this study is the consideration of all GMMs in the logic tree and investigation into how non-ergodic site-response adjustments can be applied in such a framework. Subsequent sections focus on the average site-to-site residual between GMMs, $\overline{\delta S_2 S_s}$, rather than that of individual models.

The rationale for calculating and presenting these average site terms is to retain the natural between-model variability, which partially accounts for the epistemic uncertainty in the ground-motion modeling process. In the weights-on-models logic tree approach of hazard predictions, if a site term for a specific site and model pair is used as an adjustment to the mean prediction for each model, the resulting between-model variability will be heavily reduced. This suppressed variability is not desirable and will likely partially carry into scenarios that dominate the hazard, which are outside the data set considered here. This between-model variability is retained by using the mean site term as an adjustment to all models.

Average and standard deviation of $\overline{\delta S_2 S_s}$ for all sites in the Wellington region

In Figure 5, it was illustrated that, for two basin sites, the site-to-site residuals indicate relative underprediction at approximately $T = 0.5 - 2$ s. To rule out that this is a regional bias, specific to the entire Wellington region (i.e., Figure 3), site terms for all sites in Wellington (in comparison with those for all sites in NZ) are plotted together in Figure 7. Because the residual partitioning (Equation 2) is performed for the NZ-wide data set, the average site-to-site residual is zero at all periods for all sites in Figure 7a, but not for the Wellington subset in Figure 7b. Nonetheless, the average of all site terms from the Wellington region is relatively small, with a maximum deviation of approximately -0.25 units for $T \approx 3$ s and a 68% confidence interval, graphically depicted by the $\overline{\delta S_2 S_s} \pm \phi_{S_2 S_s}$ range, which encompasses zero for all periods. Hence, in general, we see no significant regional bias in Wellington sites when all sites of all geomorphic categories are combined.

To further interrogate site residuals in Wellington, site-to-site terms can be examined by geomorphic category to explore causative features not captured by the site-response models. Figure 8 plots the average and standard deviation of site-to-site residuals for basin, basin-edge, valley, and hill sites. This illustrates that basin sites are the only category where the average site response is underpredicted for $T = 0.5 - 2$ s, with a maximum residual of ~ -0.25 natural log units at $T \approx 0.8$ s. The site periods, T_0 , for most basin sites fall within this $T = 0.5 - 2$ s period range (Table 1), so this average underprediction is consistent with the underprediction observed near the site period for two example basin sites in Figure 5. Outside this period range, the average site response for basin sites is overpredicted with a minimum value of ~ -0.25 units at $T \approx 0.1$ s. All other categories and the combination of all sites have average residuals close to zero around $T = 1$ s. For $T = 2 - 5$ s, the valley sites

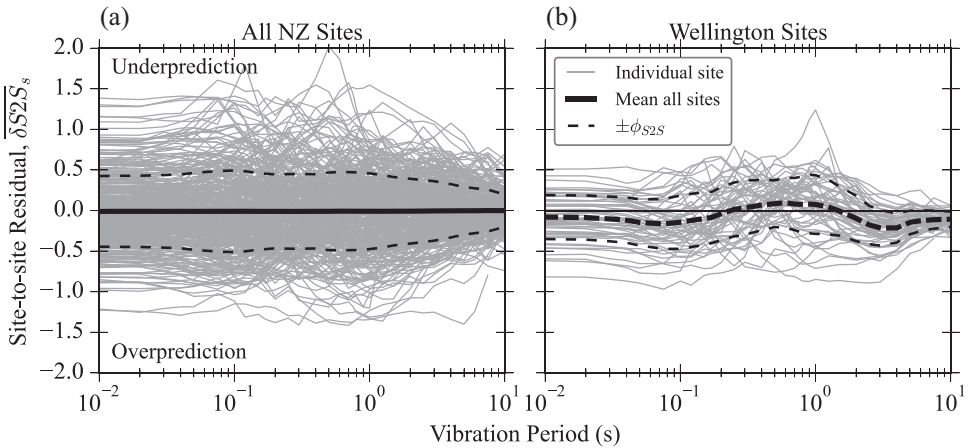


Figure 7. Weighted average site-to-site residuals, $\overline{\delta S_{2S}}$, as a function of period for (a) all sites in New Zealand and (b) sites in the Wellington region. The residual partitioning was performed for the entire NZ-wide database, which is why the average for each period is non-zero for the Wellington subset.

demonstrate significant overprediction relative to all other categories with a minimum value of ~ -0.4 units at $T \approx 3$ s. This may be because the V_{S30} -based site scaling and basin response scaling in GMMs are constrained on data from substantially larger basins. Large basins produce amplification over a wide period range, extending into longer periods, as opposed to the shallower and narrower valleys in Wellington which produce narrowband amplification close to their correspondingly shorter site period.

The segregation of mean site-to-site residuals by geomorphic categories in Figure 8 also illustrates that the site-to-site standard deviation is reduced for basin sites, and to a lesser extent valley sites, compared with all sites together. This is because the nature of the site response for these basin sites is relatively similar between sites compared with other categories, such as hill and basin-edge sites, for which there is significantly higher variability between-site responses. This is shown in Figure A.2 in the Online Supplemental Material where site terms for individual basin sites resemble one another given that the sites are all within similar basins. Figure A.2 in the Online Supplemental Material also shows the higher variability between hill sites which may be complicated due to topographic effects that can amplify or deamplify ground motions at different periods depending on the local concavity and size of the topographic feature (e.g., Rai et al., 2017).

Overall model bias and components of standard deviation

To continue the discussion in the previous subsection regarding the differences in bias between subsets of data (e.g., all NZ sites versus Wellington sites only), residual partitioning was performed for different subsets of the ground-motion database. Previously, and in all other figures outside of this subsection, results are based on residuals from a NZ-wide regression analysis. In this section, the residual analysis via Equation 2 was also performed for both Wellington sites only and Wellington basin sites only (i.e., basin, basin-edge, and valley categories) to understand the sensitivity of residuals and their uncertainties to the region and data set considered. When performing the Wellington region regressions, the between-event residuals (δB_e^m) were not constrained using the NZ-wide regression;

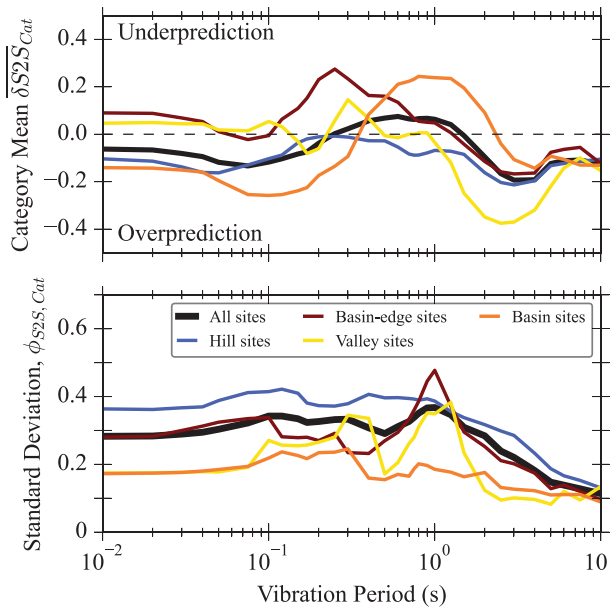


Figure 8. Category mean and standard deviation of site-to-site residuals for sites grouped by geomorphic category.

therefore, we acknowledge that there may be some unforeseen trade-offs between δB_e^m and $\delta S2S_s^m$.

As suspected from inspecting the site terms of all the sites in the Wellington region in the previous subsection (i.e., in Figure 7), Figure 9 illustrates that the bias from the NZ-wide and Wellington subset regressions are not significantly different. Bias for the two Wellington subsets are nearly identical to each other, and they generally follow similar trends to the NZ-wide bias, although they deviate slightly for $T = 0.03 - 0.1$ s, with a maximum difference of ~ 0.25 natural log units at ~ 0.08 s. This confirms that there is not significant bias for the Wellington region relative to the rest of the country, but also in an absolute sense.

Figure 10 plots the three components of standard deviation and the total standard deviation (Equation 3). Specifically, these components are the between-event ($\bar{\tau}$), site-to-site ($\bar{\phi}_{S2S}$), single-station ($\bar{\phi}_{SS}$), and total ($\bar{\sigma}_T$) standard deviations. The overlines indicate that these values are averaged over all GMMs considered, as the residual calculation is performed for each model separately. As expected from existing literature (e.g., Sung and Abrahamson, 2022), the site-response variability components $\bar{\phi}_{S2S}$ and $\bar{\phi}_{SS}$ are lower when a smaller region (i.e., Wellington only) is considered. $\bar{\phi}_{S2S}$ and $\bar{\phi}_{SS}$ for the Wellington-only data sets are approximately 50% lower than those from the NZ-wide data set where all regions in NZ are combined. This reduction in variability for a smaller region highlights one of the issues with global models, which combine ground motions from different regions. Even for a relatively small region like NZ, there are distinct ground-motion characteristics between different sub-regions, creating an inflated aleatory variability when they are combined. Such reductions in the total sigma can have significant implications for the hazard computed via PSHA (e.g., Abrahamson et al., 2019; Anderson and Brune, 1999; Bommer and Abrahamson, 2006).

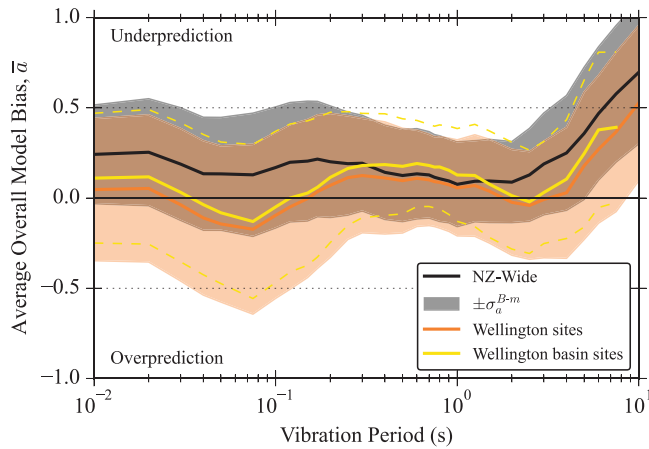


Figure 9. Mean overall model bias across all GMMs ($\bar{\tau}$) for three data sets. The mixed-effects regression was performed on the NZ-wide database and on subsets including all sites in Wellington, and basin sites in Wellington (i.e., basin, basin-edge, and valley categories). The $\pm\sigma$ for Wellington basin sites is shown in dashed yellow lines.

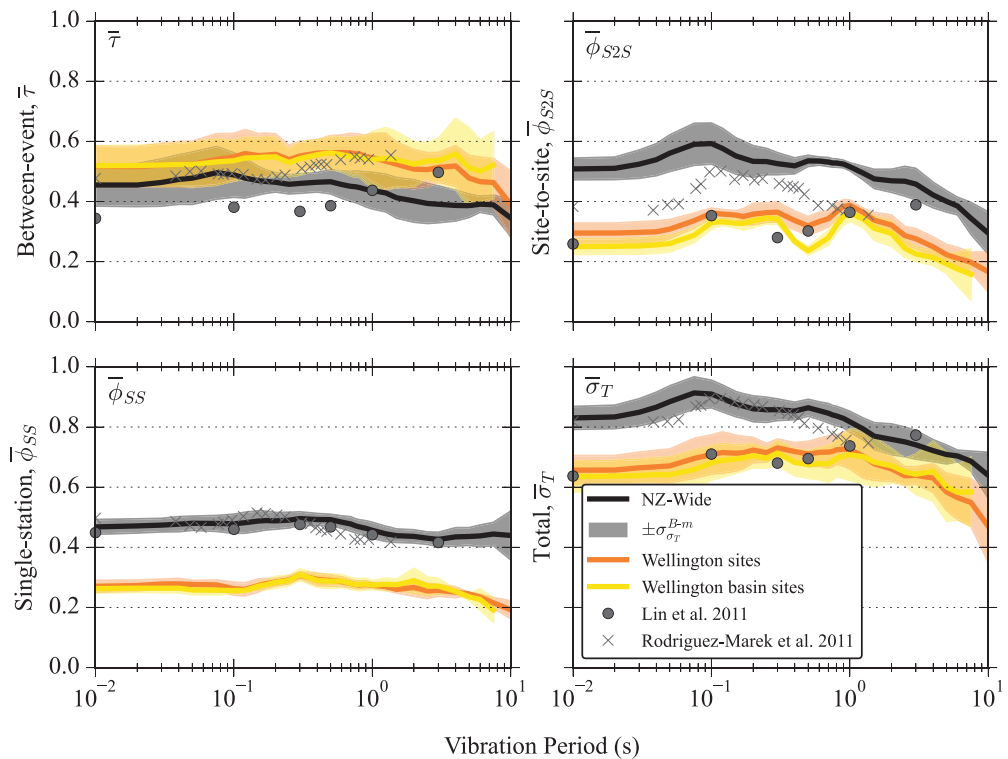


Figure 10. Standard deviations from the mixed-effects regression, averaged across all GMMs, including the between-event (τ), site-to-site (ϕ_{S2S}), single-station (ϕ_{SS}), and total standard deviations (σ_T). As in Figure 9, the regression was performed on the NZ-wide database, a subset including all sites in Wellington, and a subset including only basin sites in Wellington.

As a comparison, Figure 10 also includes standard deviation estimates from two published papers focusing on single-station standard deviation in other regions of the world (Japan and Taiwan, respectively; Lin et al., 2011; Rodriguez-Marek et al., 2011). The values obtained from the residual analysis in this study are similar to these other studies, suggesting that the performance of GMMs in NZ is comparable to other regions. We note that the estimates of residuals at long periods (e.g., $T > 7$ s) are more uncertain, given the relatively few number of records that have maximum useable periods up to 10 s. For this reason, the results from the Wellington basin sites in Figures 9 and 10 do not extend to $T = 10$ s.

Dependence of residuals on site characteristics

To further understand causative parameters for site response and the observed patterns in residuals, it is useful to determine whether the site residuals are dependent on any easily attainable or already-available site parameters. The dependence on site residuals on four site parameters is investigated in Figure 11 for Wellington basin sub-regions (i.e., excluding hill sites). The residual is quantified using three simple metrics: T_{res} , the period at which the maximum of $\overline{\delta S^2 S_s}$ occurs; and $\overline{\delta S^2 S_s}(T = T_{res})$ and $\overline{\delta S^2 S_s}(T = T_0)$, which are the values of $\overline{\delta S^2 S_s}$ at T_{res} and T_0 , respectively. The dependence of each of these metrics to the following site parameters is assessed: V_{S30} , T_0 , $Z_{1.0}$, and the closest distance to the basin edge ($D_{basin-edge}$), which was calculated as the shortest Euclidean distance between the site and the basin-edge trace. A linear regression is performed for each relationship to determine whether there is any statistically significant correlation between the site parameters and the residual metrics.

The top panels in Figure 11 show that T_0 and $Z_{1.0}$ are moderately correlated to T_{res} , with Pearson's r values > 0.6 and $p \leq 0.001$. $D_{basin-edge}$ displays a slightly weaker correlation to T_{res} . These trends are complicated by the complexities discussed subsequently in the "Normalization of spectral period by site period" section (e.g., basin-edge effects in Thorndon and the double-peak in Lower Hutt, for which the shorter period peak often dominates). V_{S30} shows no correlation with any residual metrics, which is not unexpected given that the GMMs use V_{S30} to quantify site effects, and therefore, the residuals should be unbiased with regard to V_{S30} . Interestingly, $Z_{1.0}$ is also considered in crustal GMMs; however, the site residuals are not unbiased relative to this term. This suggests that the basin response terms in GMMs, based on $Z_{1.0}$, are not performing well in New Zealand. This may be because the global versions of these models are heavily influenced by data from California (Seyhan and Stewart, 2014), including many records from the Los Angeles basin which is significantly larger and deeper than the basins and valleys in New Zealand. The $Z_{1.0}$ measurements are also not well constrained, as few sites in Wellington have boreholes and invasive V_S measurements to bedrock (Wotherspoon et al., 2023).

The amplitude of $\overline{\delta S^2 S_s}$ does not appear to display any significant correlation with any of these site parameters (bottom two rows of Figure 11). The peak positive value in the site residuals $[\overline{\delta S^2 S_s}(T = T_{res})]$, corresponding to underprediction, has a mean value of ≈ 0.45 log units across all basin and valley sites in Wellington. The residual values at T_0 are close to these peak values.

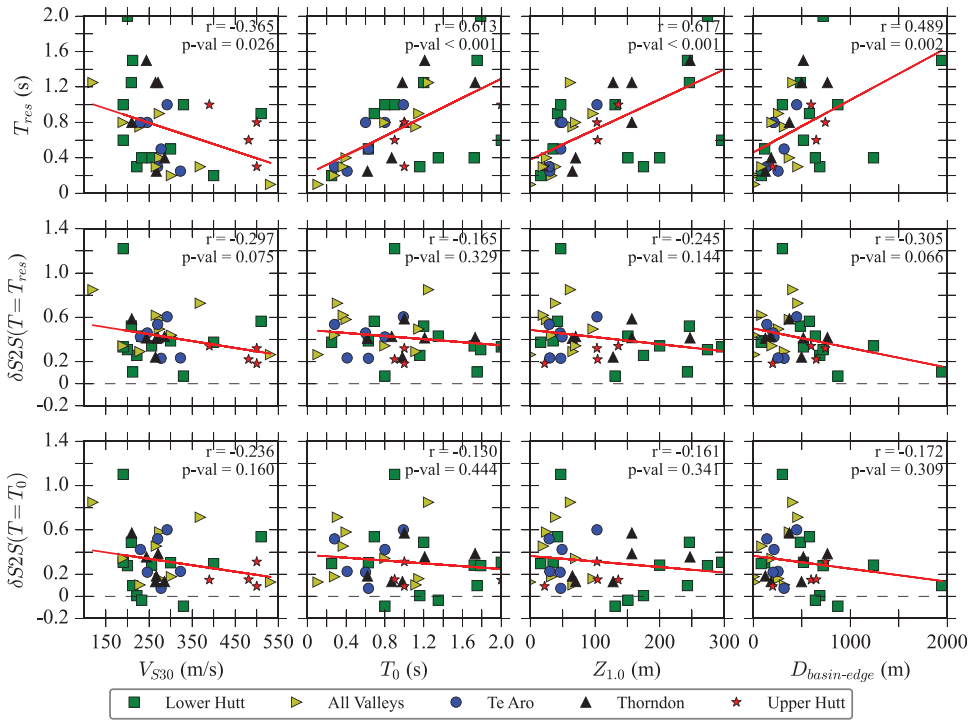


Figure 11. Dependence of three residual metrics $[T_{res}, \delta S2S(T = T_{res}), \delta S2S(T = T_0)]$, on four site parameters (V_{S30} , T_0 , $Z_{1.0}$, $D_{basin-edge}$) for basin and valley sites (i.e., hill sites are excluded). Sites are identified based on region. A linear regression is performed for each panel to identify trends and dependences on any parameters. Pearson's r correlation coefficients and p values for each regression are shown in every panel.

Regionalization of site terms

The site-to-site residuals, $\delta S2S_s$, can be used in site-specific adjustments to GMMs; however, this study aims to understand site-response trends more broadly across the region. This is useful for forward prediction applications, in which ground motions and site response have not been instrumentally measured. To understand such regional trends, the weighted means and between-model standard deviations of $\delta S2S_s^m$ (i.e., $\overline{\delta S2S_s}$ and $\sigma_{S2S,s}^{B-m}$ as defined by Equations 6 and 7) are regionalized and presented in Figure 12 as a function of vibration period. Each column of Figure 12 includes the site terms for one of the four basin sub-regions of Te Aro, Thorndon, Lower Hutt, and Upper Hutt (Figure 3). The top row of panels presents $\overline{\delta S2S_s}$ and the bottom panels $\sigma_{S2S,s}^{B-m}$ for each site in the region. The regional mean ($\overline{\delta S2S_R}$; Equation 8) and standard deviation ($\phi_{S2S,R}$; Equation 9) are also included in the respective panel for each region. The regional means generally show underprediction in the period range of $T = 0.5 - 2$ s for all regions, with peaks in the mean residuals of approximately $0.16 - 0.26$ lognormal units. For $T > 2.5$ s, all basin regions display some overprediction with fairly constant mean residual values of approximately -0.1 to -0.25 . The Te Aro and Upper Hutt regions also display average overprediction for $T < 0.3$ s. The maximum error in these average residuals occurs in the Te Aro region at $T \approx 0.1$ s with a value of -0.39 , corresponding to overprediction.

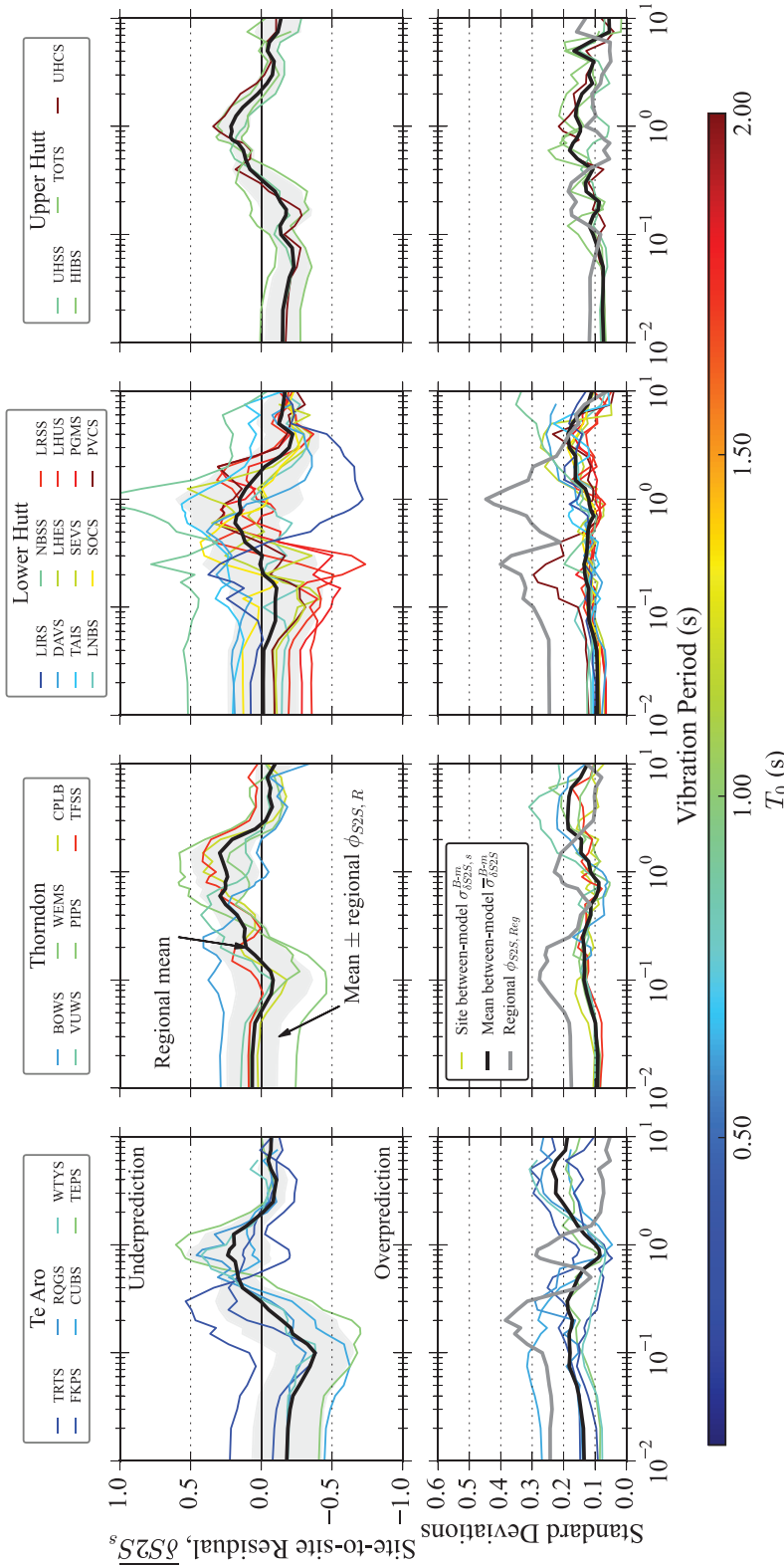


Figure 12. Site-to-site residuals and standard deviations for four basin sub-regions (Te Aro, Thorndon, Lower Hutt, and Upper Hutt) as a function of vibration period. Top panels: mean site-to-site residuals, $\delta S2S_s$, for all sites within each of the basin sub-regions, and the regional mean for each region. Bottom panels: between-model standard deviations for each site, and site-to-site standard deviations for each region. Individual site lines are color-coded by site period (T_0).

The average underprediction for $T=0.5-2$ s in all regions is not unexpected, given that this is the period range at which the Wellington basin has been observed to strongly amplify ground motions. Figure 12 shows relatively low between-model standard deviations (i.e., $\sigma_{\delta S2S,s}^{B-m}$ of approximately 0.1–0.2), suggesting fairly good agreement between the site terms of all the models considered in this study, as shown previously in Figures 5 and 6. However, the regional site-to-site standard deviations ($\phi_{S2S,R}$) reach high values of 0.3 to 0.5 at their peaks (Figure 12). Importantly, these peaks in $\phi_{S2S,R}$ generally occur at the period range of interest for basin effects in Wellington (i.e., close to $T=1$ s). This suggests that sites within the same sub-basin experience amplification (or underprediction) at different periods and different site parameters should be further investigated to identify any correlations between the shape of the site terms and site characteristics.

The results for valleys are regionalized in Figure A.3 of the Online Supplemental Material. This shows that the peaks in residuals of individual sites are pronounced and occur over a narrower frequency band than the basin sites. These pronounced narrow peaks, that generally occur at different periods for different sites, result in a high regional standard deviation, $\phi_{S2S,R}$.

Normalization of spectral period by site period

Previous work in Wellington has illustrated that patterns of basin/site amplification are consistent with patterns of site period estimates, and that site period may be a good predictor for site response (de la Torre et al., 2024; Kaiser et al., 2023). Other studies have leveraged off this dependence on site period and had success with incorporating site period into empirical site-response models (e.g., Hassani and Atkinson, 2018; Héloïse et al., 2012; Kwak et al., 2017). Figure 11 demonstrated a reasonably strong correlation between T_0 and the period at which the peak residual (i.e., the maximum underprediction) occurs. To further elucidate this trend, vibration periods at which $\delta S2S$ was calculated were normalized by the site period of each site. Figure 13 plots the same regionally segregated $\delta S2S$ plotted in Figure 12, albeit as a function of normalized period (T/T_0). Figure 14 plots regionalized site terms versus normalized period for the valley sub-regions. T_0 estimates used in this study are taken directly from the NZ GMDDB (Hutchinson et al., 2022) and are generally based on earthquake and microtremor horizontal-to-vertical spectral ratio (eHVSR and mHVSR, respectively; Wotherspoon et al., 2023). We note that because eHVSR is derived from earthquake ground motions, some T_0 estimates cannot be considered as an independent parameter for the prediction of site response. However, exclusion of these values would result in less T_0 estimates; therefore, all T_0 estimates are used in this study.

For many sub-basins, there appears to be consistency between the various sites $\overline{\delta S2S_s}$, when period is normalized. That is, most sites generally display underprediction at or near the site period. This is especially true for Te Aro and Lower Hutt basin sub-regions (Figure 13) and all valley sub-regions (Figure 14). The regionalized site terms are influenced by the following complexities: In Thorndon, site VUWS is a complicated site on the edge of a steep drop-off in bedrock at which the site response and/or site period estimate may be influenced by complex multidimensional site response. Both VUWS and BOWS are also closer to the basin edge compared with the other sites in Thorndon and therefore may be influenced by other phenomena not captured by the GMMs or the site period estimate (e.g., basin-edge effects). Lower Hutt sites display strong site amplification not only at the fundamental site period but also at a shorter period peak, which is likely

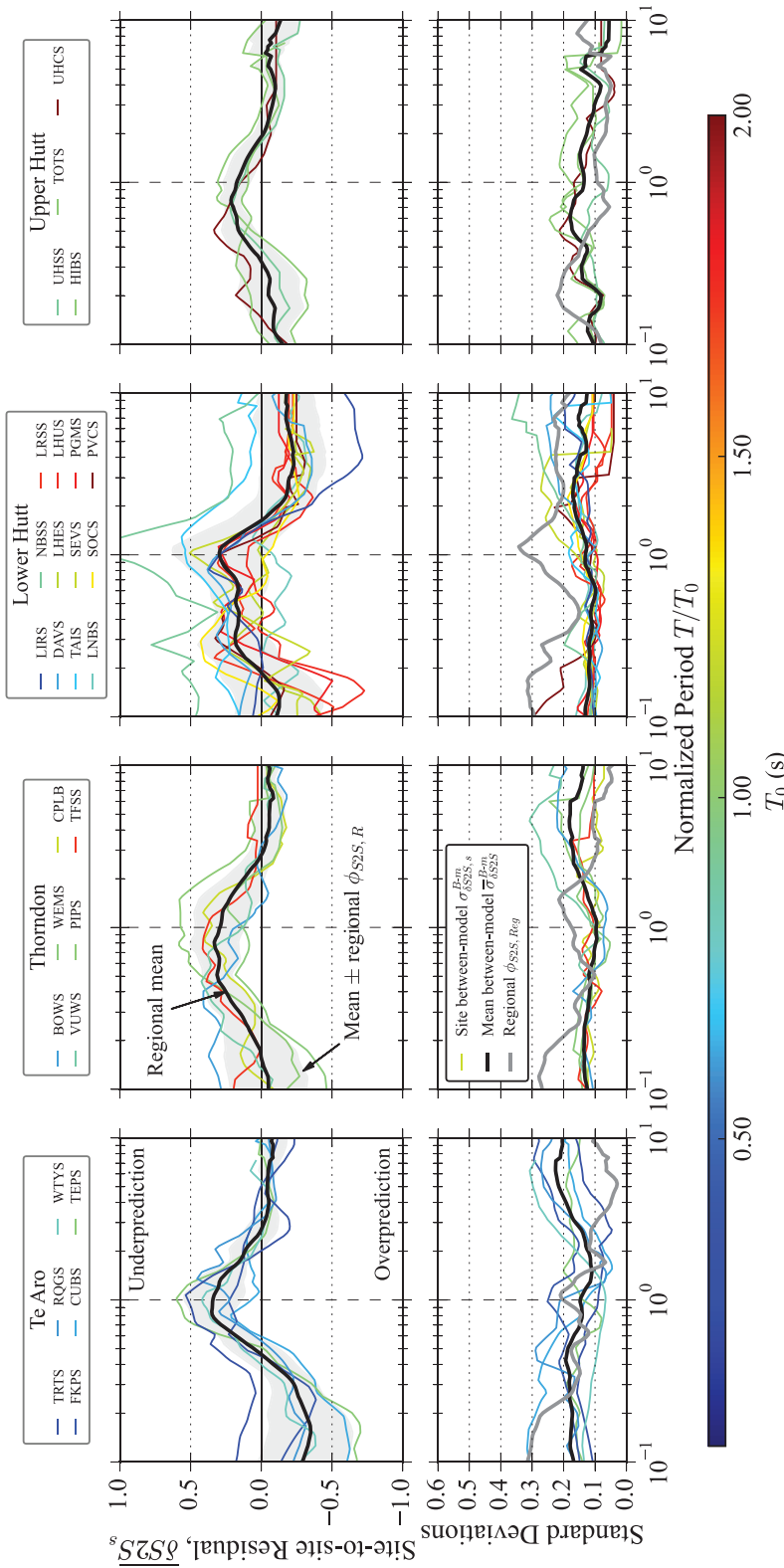


Figure 13. Site-to-site residuals and standard deviations for four basin regions (Te Aro, Thorndon, Lower Hutt, and Upper Hutt) as a function of normalized period (i.e., T/T_0). Top panels: mean site-to-site residuals, $\delta S2S_s$, for all sites within each of the basin sub-regions, and the regional mean for each region. Bottom panels: between-model standard deviations for each site, and regional site-to-site standard deviation $\phi_{S2S,Reg}$. Individual site lines are color-coded by site period (T_0).

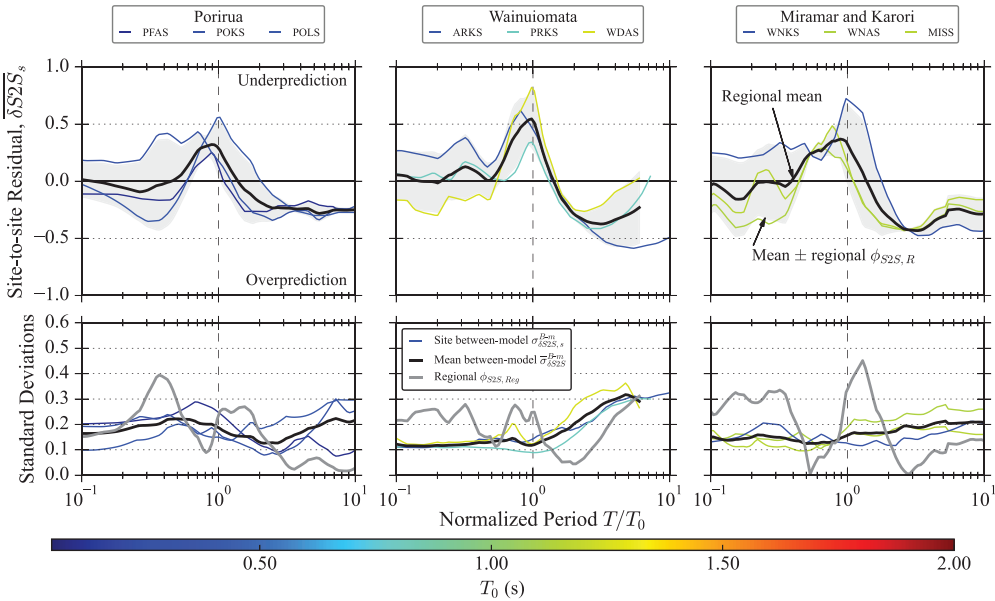


Figure 14. Site-to-site results and standard deviations for three valley regions (Porirua, Wainuiomata, and Miramar and Karori) as a function of normalized period (i.e., T/T_0). Top panels: mean site-to-site residuals, δS_{2S_s} , for all sites within each of the basin sub-regions, and the regional mean for each region. Bottom panels: between-model standard deviations for each site, and regional site-to-site standard deviation $\phi_{S_{2S_s}, Reg}$. Individual site lines are color-coded by site period (T_0).

representative of a shallower impedance contrast. This “double-peak” is visible in many individual site curves and, to a lesser extent, in the regional mean.

In general, normalization by site period results in a significant reduction in the regional between-site standard deviation. For most regions, the maximum regional standard deviation drops from about 0.3 – 0.55 to 0.25 – 0.4 in natural log units. Again, the benefits of normalizing by site period at Te Aro are illustrated by the standard deviation which drops from a maximum of about 0.4 to about 0.3. This suggests that an adjustment factor conditioned on site period could perform better than a model that is independent of site period (e.g., Figure 12).

Comparison of correlation-based versus site-specific $Z_{1.0}$ and $Z_{2.5}$

The results in this article are more likely to be used on a site-specific basis, where PSHA is applied to an individual site or project, as opposed to a nationwide PSHA, like the NZ NSHM. In these site-specific applications, typically, best estimates of site-specific basin-depth terms, $Z_{1.0}$ and $Z_{2.5}$, would be used. The results presented in this article are for GMM predictions and residual analyses using site-specific estimates of $Z_{1.0}$ and $Z_{2.5}$ from the NZ GMDB (i.e., Hutchinson et al., 2022; Wotherspoon et al., 2023). In the NZ NSHM, default values of the basin-depth terms, $Z_{1.0}$ and $Z_{2.5}$, based on V_{S30} correlations were used (Bradley et al., 2024; Kaiser et al., 2023). The Chiou and Youngs (2014) $V_{S30} - Z_{1.0}$ correlation and the Campbell and Bozorgnia (2014) $V_{S30} - Z_{2.5}$ correlation were used for all relevant GMMs. This is not uncommon in NSHMs around the world (e.g., USA NSHM), as the hazard is generally calculated using different values of V_{S30}

(with the corresponding basin-depth terms) for the whole country rather than using spatially varying estimates of V_{S30} , $Z_{1.0}$, and $Z_{2.5}$. The 2018 USA NSHM did, however, use site-specific estimates of basin-depth terms for the following four deep basin regions when $Z_{2.5} > 3$ km: Seattle, Los Angeles, San Francisco, and Salt Lake City (Petersen et al., 2020). In this study, we also performed the GMM predictions and residual analyses using correlation-based estimates of $Z_{1.0}$ and $Z_{2.5}$ and compared the results from correlation-based and site-specific values in this subsection.

The site-specific estimates of $Z_{1.0}$ and $Z_{2.5}$ in the Wellington region are significantly lower than the default value calculated using V_{S30} -based correlations. These higher values of $Z_{1.0}$ obtained from V_{S30} -based correlations result in higher predictions of spectral acceleration at long periods. Given that the average bias for the whole country and the Wellington region (Figure 9) shows underprediction at $T > 5$ s, the NZ NSHM used the V_{S30} -based correlations instead of site-specific estimates. This approach is generally consistent with the 2018 USA NSHM, which generally only uses site-specific basin-depth values if they result in amplification relative to the default V_{S30} -based values.

Figure 15 plots regional mean site-to-site residuals and standard deviations for all basin and valley sub-regions as a function of normalized period and compares predictions that used correlation-based values of $Z_{1.0}$ and $Z_{2.5}$ with those that used site-specific estimates. This figure illustrates that the influence of this assumption on the site terms is small, albeit,

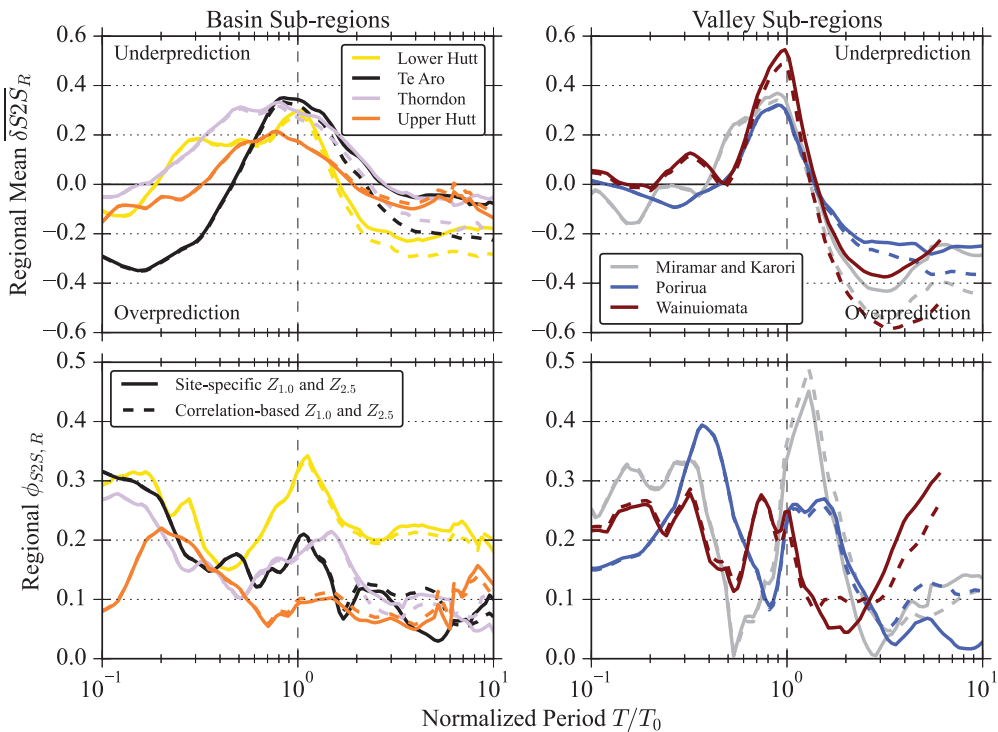


Figure 15. Regional mean site-to-site residuals and standard deviations versus normalized period for all basin and valley sub-regions considered. Predictions that use site-specific estimates of basin-depth terms ($Z_{1.0}$ and $Z_{2.5}$) from the NZ GMDB (solid lines) are compared with predictions that use V_{S30} -correlation-based basin-depth terms (dashed lines).

there are higher long-period amplitudes for the generic values (solid lines) compared with the site-specific values (dashed lines), as expected. However, some of this additional long-period amplification is absorbed by the bias term. For this reason, in a similar format, Figure A.4 in the Online Supplemental Material plots the regional systematic site terms ($\overline{a + \delta S2S_R}$) and standard deviations ($\phi_{(a + \delta S2S), R}$) versus period. With the bias term included (Figure A.4 in the Online Supplemental Material), the overall influence of the basin-depth term is more pronounced. For all regions, the generic terms result in slightly greater amplification for $T > 1$ s. While this generally results in less underprediction for basin sites, it results in greater overprediction for valley sites for $T = 1 - 5$ s.

Importantly, the shape of the regional site terms, in normalized period space (Figure 15), is similar between all basin sub-regions and all valley sub-regions. However, the general shape for basin sub-regions is different to that of valley sub-regions. This highlights that similar geomorphic features in the same region may have similar average site responses, and that the distinction between basin and valley sites proposed by Nweke et al. (2022) is useful.

Conclusion

This article analyzed ground-motion residuals for the Wellington region to assess the performance of empirical GMMs used in the 2022 NZ NSHM revision. Specifically, the site-to-site residuals ($\delta S2S$), or “site terms,” for sites in Wellington were closely inspected to judge the GMMs in their ability to predict site effects attributed to sedimentary basins. Site terms from all the GMMs considered in the NSHM were evaluated to quantify the between-model epistemic uncertainty. Then, site terms were grouped geographically by specific basin or valley sub-regions, and by general geomorphic categories (basin, basin edge, valley, and hill). The dependence of these site terms on various site characterization parameters and on tectonic type was also assessed.

The between-model variability in site-to-site residuals ($\delta S2S$) was found to be relatively small, generally $\sim 0.05 - 0.1$ natural log units for GMMs within the same tectonic type and $\sim 0.15 - 0.2$ across all GMMs of all tectonic types (Figure 6). When overall model bias is considered, the between-model variability increases drastically to $\sim 0.3 - 0.5$ in natural log units when considering all GMMs. This suggests that the differences in the site-response models between different GMMs are relatively small compared with other components of the GMMs. These values of model-to-model variability across all GMMs are reasonable estimates of epistemic model uncertainty that could be used with back-bone-type GMMs (e.g., Bommer, 2012; Stafford, 2022).

When all sites from all geomorphic categories in the Wellington region are combined, no significant systematic bias is observed relative to the rest of the country. However, when segregated into different categories, a clear underprediction is observed for basin sites at periods of $0.5 - 2$ s. This underprediction is attributed to the models' inability to capture strong resonance in site response of sedimentary basins in Wellington. Further separation into individual geomorphological features, such as separate basins and valleys, shows that different sub-regions can have unique site-response characteristics. Most basin and valley regions demonstrate the maximum underprediction over a period range centered around the site period (T_0), suggesting that T_0 could be used to better constrain the site response of sedimentary basin sites.

This study identified basin-specific systematic trends in bias and imprecision, based on mean site-to-site residuals, for the following basins and valleys in the Wellington region: Te Aro, Thorndon, Lower Hutt, Porirua, Wainuiomata, Miramar, and Karori. These residual trends form the basis for the development of adjustment factors to the mean site-response model within GMMs, to create partially non-ergodic GMMs for use in PSHA. Further work is required to fully develop and test the framework for application of these adjustment factors to PSHA in the Wellington region.

Acknowledgments

All members of the NZ NSHM ground-motion characterization modeling and Wellington Basin sub-groups and the Technical Advisory Group are gratefully acknowledged for their input and participation throughout the duration of the project.

Declaration of conflicting interests

The author(s) declared no potential conflicts of interest with respect to the research, authorship, and/or publication of this article.

Funding

The author(s) disclosed receipt of the following financial support for the research, authorship, and/or publication of this article: The authors thank the New Zealand National Seismic Hazard Model (NSHM) update program, the New Zealand Earthquake Commission (EQC), and QuakeCoRE, a New Zealand Tertiary Education Commission-funded Centre, for funding this work. This is QuakeCoRE publication ID 955.

ORCID iDs

Christopher A de la Torre  <https://orcid.org/0000-0002-7946-7812>

Brendon A Bradley  <https://orcid.org/0000-0002-4450-314X>

Robin L Lee  <https://orcid.org/0000-0003-1033-5923>

Liam Wotherspoon  <https://orcid.org/0000-0002-4883-5328>

Supplemental material

Supplemental material for this article is available online.

Data and resources

The Hutchinson et al. (2022) NZ GMDB files are publicly available at: https://osf.io/q9yrg/?view_only=05337ba1ebc744fc96b9924de633ca0e. The following versions of the GMDB were used for this study: the site table from Version 3.2 for site parameters and the ground-motion IMs table from Version 1 with IMs from Version 3.2 for the site CPLB.

References

- Abrahamson NA and Gülerce Z (2020) *Regionalized ground-motion models for subduction earthquakes based on the NGA-SUB database*. Technical report 2020/25, 5 December. Berkeley, CA: Pacific Earthquake Engineering Research Center.
- Abrahamson NA, Kuehn NM, Walling M and Landwehr N (2019) Probabilistic seismic hazard analysis in California using nonergodic ground-motion models. *Bulletin of the Seismological Society of America* 109: 1235–1249.

- Abrahamson NA, Silva WJ and Kamai R (2014) Summary of the ASK14 ground motion relation for active crustal regions. *Earthquake Spectra* 30: 1025–1055.
- Adams B, Davis R, Berrill J and Taber J (2012) Two-dimensional site effects in Wellington and the Hutt Valley similarities to Kobe. *Research report, Department of Civil Engineering, University of Canterbury, Christchurch, New Zealand*, February.
- Al Atik L, Abrahamson N, Bommer JJ, Scherbaum F, Cotton F and Kuehn N (2010) The variability of ground-motion prediction models and its components. *Seismological Research Letters* 81: 794–801.
- Anderson JG and Brune JN (1999) Probabilistic seismic hazard analysis without the ergodic assumption. *Seismological Research Letters* 70: 19–28.
- Atkinson GM (2006) Single-station sigma. *Bulletin of the Seismological Society of America* 96: 446–455.
- Atkinson GM (2022) *Backbone ground-motion models for crustal, interface, and slab earthquakes in New Zealand*. GNS Science Consultancy Report 2022/11, April. Lower Hutt, New Zealand: GNS Science.
- Baker J, Bradley B and Stafford P (2021) *Probabilistic Seismic Hazard and Risk Analysis*. Cambridge: Cambridge University Press.
- Bommer JJ (2012) Challenges of building logic trees for probabilistic seismic hazard analysis. *Earthquake Spectra* 28: 1723–1735.
- Bommer JJ and Abrahamson NA (2006) Why do modern probabilistic seismic-hazard analyses often lead to increased hazard estimates? *Bulletin of the Seismological Society of America* 96: 1967–1977.
- Boore DM (2010) Orientation-independent, nongeometric-mean measures of seismic intensity from two horizontal components of motion. *Bulletin of the Seismological Society of America* 100: 1830–1835.
- Boore DM, Stewart JP, Seyhan E and Atkinson GM (2014) NGA-West2 equations for predicting PGA, PGV, and 5% damped PSA for shallow crustal earthquakes. *Earthquake Spectra* 30: 1057–1085.
- Bozorgnia Y, Abrahamson NA, Ahdi SK, Ancheta TD, Atik LA, Archuleta RJ, Atkinson GM, Boore DM, Campbell KW, Chiou BS-J, Contreras V, Darragh RB, Derakhshan S, Donahue JL, Gregor N, Gulerce Z, Idriss I, Ji C, Kishida T, Kottke AR, Kuehn N, Kwak D, Kwok AO-L, Lin P, Macedo J, Mazzoni S, Midorikawa S, Muin S, Parker GA, Rezaeian S, Si H, Silva WJ, Stewart JP, Walling M, Wooddell K and Youngs RR (2022) NGA-subduction research program. *Earthquake Spectra* 38: 783–798.
- Bozorgnia Y, Abrahamson NA, Atik LA, Ancheta TD, Atkinson GM, Baker JW, Baltay A, Boore DM, Campbell KW, Chiou BS-J, Darragh R, Day S, Donahue J, Graves RW, Gregor N, Hanks T, Idriss IM, Kamai R, Kishida T, Kottke A, Mahin SA, Rezaeian S, Rowshandel B, Seyhan E, Shahi S, Shantz T, Silva W, Spudich P, Stewart JP, Watson-Lamprey J, Wooddell K and Youngs R (2014) NGA-West2 research project. *Earthquake Spectra* 30: 973–987.
- Bradley BA (2013) A New Zealand-specific pseudospectral acceleration ground-motion prediction equation for active shallow crustal earthquakes based on foreign models. *Bulletin of the Seismological Society of America* 103: 1801–1822.
- Bradley BA (2015) Systematic ground motion observations in the Canterbury earthquakes and region-specific non-ergodic empirical ground motion modeling. *Earthquake Spectra* 31: 1735–1761.
- Bradley BA, Bora SS, Lee RL, Manea EF, Gerstenberger MC, Stafford PJ, Atkinson GM, Weatherill G, Hutchinson J, de la Torre CA, Hulsey AM and Kaiser AE (2024) The ground-motion characterization model for the 2022 New Zealand National Seismic Hazard Model. *Bulletin of the Seismological Society of America* 114: 329–349.
- Bradley BA, Wotherspoon LM, Kaiser AE, Cox BR and Jeong S (2018) Influence of site effects on observed ground motions in the Wellington Region from the Mw 7.8 Kaikōura, New Zealand, Earthquake. *Bulletin of the Seismological Society of America* 108: 1722–1735.
- Campbell KW and Bozorgnia Y (2014) NGA-West2 ground motion model for the average horizontal components of PGA, PGV, and 5% damped linear acceleration response spectra. *Earthquake Spectra* 30: 1087–1115.

- Chiou BS and Youngs RR (2014) Update of the Chiou and Youngs NGA model for the average horizontal component of peak ground motion and response spectra. *Earthquake Spectra* 30: 1117–1153.
- de la Torre C, Bradley B, Kuncar F, Lee R, Wotherspoon L and Kaiser A (2024) Combining observed linear basin amplification factors with 1D nonlinear site-response analyses to predict site response for strong ground motions: Application to Wellington, New Zealand. *Earthquake Spectra* 40: 143–173.
- Gerstenberger MC, Bora S, Bradley BA, Dicaprio C, Kaiser A, Manea EF, Nicol A, Rollins C, Stirling MW, Thingbaijam KK, Van Dissen RJ, Abbott ER, Atkinson GM, Chamberlain C, Christophersen A, Clark K, Coffey GL, de la Torre CA, Ellis SM, Fraser J, Graham K, Griffin J, Hamling IJ, Hill MP, Howell A, Hulsey A, Hutchinson J, Iturrieta P, Johnson KM, Jurgens VO, Kirkman R, Langridge RM, Lee RL, Litchfield NJ, Maurer J, Milner KR, Rastin S, Rattenbury MS, Rhoades DA, Ristau J, Schorlemmer D, Seebeck H, Shaw BE, Stafford PJ, Stolte AC, Townend J, Villamor P, Wallace LM, Weatherill G, Williams CA and Wotherspoon LM (2024) The 2022 Aotearoa New Zealand National Seismic Hazard Model: Process, overview, and results. *Bulletin of the Seismological Society of America* 114: 7–36.
- Hassani B and Atkinson GM (2018) Site-effects model for central and eastern North America based on peak frequency and average shear-wave velocity. *Bulletin of the Seismological Society of America* 108: 338–350.
- Héloïse C, Bard P-Y, Duval A-M and Bertrand E (2012) Site effect assessment using KiK-net data: Part 2—Site amplification prediction equation based on f_0 and V_{sz} . *Bulletin of Earthquake Engineering* 10: 451–489.
- Hutchinson J, Bradley B, Lee R, Wotherspoon L, Dupuis M, Schill C, Motha J, Kaiser A and Manea E (2022) *2021 New Zealand strong ground motion database*. GNS Science Report 2021/56, September. Lower Hutt, New Zealand: GNS Science.
- Kaiser AE, Hill MP, de la Torre C, Bora S, Manea E, Wotherspoon L, Atkinson GM, Lee R, Bradley B, Hulsey A, Stolte A and Gerstenberger M (2023) Overview of site effects and the application of the 2022 New Zealand NSHM in the Wellington basin, New Zealand. *Bulletin of the Seismological Society of America* 114: 399–421.
- Kaiser AE, Hill MP, McVerry G, Bourguignon S, Bruce Z, Morgenstern R, Giallini S and Wotherspoon L (2020) Wellington's sedimentary basin and its role in amplifying earthquake ground motions: New CBD 3D model and maps. In: *Proceedings of the 2020 New Zealand Society for Earthquake Engineering Annual Technical Conference*, Wellington, New Zealand, 22–24 April. Wellington, New Zealand: New Zealand Society for Earthquake Engineering.
- Kaiser AE, Manea E, Wotherspoon L, Hill M, Lee R, de la Torre C, Stolte A, Bora S, Bradley B, Hulsey A and Gerstenberger M (2022) *2022 revision of the National Seismic Hazard Model for New Zealand: Overview of site/basin effects, including a case study of the Wellington basin*. GNS Science Consultancy Report 2022/56, September. Lower Hutt, New Zealand: GNS Science.
- Kotha SR, Bindi D and Cotton F (2016) Partially non-ergodic region specific GMPE for Europe and Middle-East. *Bulletin of Earthquake Engineering* 14: 1245–1263.
- Kuehn N, Bozorgnia Y, Campbell KW and Gregor N (2020) *Partially non-ergodic ground-motion model for subduction regions using the NGA-subduction database*. Technical report 2020/04, 1 September. Berkeley, CA: Pacific Earthquake Engineering Research Center.
- Kwak DY, Stewart JP, Mandokhail SJ and Park D (2017) Supplementing VS30 with H/V spectral ratios for predicting site effects. *Bulletin of the Seismological Society of America* 107: 2028–2042.
- Landwehr N, Kuehn NM, Scheffer T and Abrahamson N (2016) A nonergodic ground-motion model for California with spatially varying coefficients. *Bulletin of the Seismological Society of America* 106: 2574–2583.
- Lavrentiadis G, Abrahamson NA, Nicolas KM, Bozorgnia Y, Goulet CA, Babič A, Macedo J, Dolšek M, Gregor N, Kottke AR, Lacour M, Liu C, Meng X, Phung V-B, Sung CH and Walling M (2023) Overview and introduction to development of non-ergodic earthquake ground-motion models. *Bulletin of Earthquake Engineering* 21(11): 5121–5150.

- Lee RL, Bradley BA, Manea E, Hutchinson J and Bora S (2024) Evaluation of empirical ground-motion models for the 2022 New Zealand National Seismic Hazard Model revision. *Bulletin of the Seismological Society of America* 114: 311–328.
- Lin P-S, Chiou B, Abrahamson N, Walling M, Lee C-T and Cheng C-T (2011) Repeatable source, site, and path effects on the standard deviation for empirical ground-motion prediction models. *Bulletin of the Seismological Society of America* 101: 2281–2295.
- Macedo J and Liu C (2022) A nonergodic ground motion model for Chile. *Bulletin of the Seismological Society of America* 112: 2542–2561.
- Nweke CC, Stewart JP, Wang P and Brandenberg SJ (2022) Site response of sedimentary basins and other geomorphic provinces in southern California. *Earthquake Spectra* 38: 2341–2370.
- Parker GA and Baltay AS (2022) Empirical map-based nonergodic models of site response in the greater Los Angeles area. *Bulletin of the Seismological Society of America* 112: 1607–1629.
- Parker GA, Stewart JP, Boore DM, Atkinson GM and Hassani B (2022) NGA-subduction global ground motion models with regional adjustment factors. *Earthquake Spectra* 38: 456–493.
- Petersen MD, Shumway AM, Powers PM, Mueller CS, Moschetti MP, Frankel AD, Rezaeian S, McNamara DE, Luco N, Boyd OS, Rukstales KS, Jaiswal KS, Thompson EM, Hoover SM, Clayton BS, Field EH and Zeng Y (2020) The 2018 update of the US National Seismic Hazard Model: Overview of model and implications. *Earthquake Spectra* 36: 5–41.
- Rai M, Rodriguez-Marek A and Chiou BS (2017) Empirical terrain-based topographic modification factors for use in ground motion prediction. *Earthquake Spectra* 33: 157–177.
- Rodriguez-Marek A, Montalva GA, Cotton F and Bonilla F (2011) Analysis of single-station standard deviation using the KiK-net data. *Bulletin of the Seismological Society of America* 101: 1242–1258.
- Rodriguez-Marek A, Rathje EM, Bommer JJ, Scherbaum F and Stafford PJ (2014) Application of single-station sigma and site-response characterization in a probabilistic seismic-hazard analysis for a new nuclear site. *Bulletin of the Seismological Society of America* 104: 1601–1619.
- Seyhan E and Stewart JP (2014) Semi-empirical nonlinear site amplification from NGAWest2 data and simulations. *Earthquake Spectra* 30: 1241–1256.
- Stafford PJ (2022) *A model for the distribution of response spectral ordinates from New Zealand crustal earthquakes based upon adjustments to the Chiou and Youngs (2014) response spectral model*. GNS Science report 2022/15, September. Lower Hutt, New Zealand: GNS Science.
- Sung C-H, Abrahamson NA, Kuehn NM, Traversa P and Zentner I (2023) A non-ergodic ground-motion model of Fourier amplitude spectra for France. *Bulletin of Earthquake Engineering* 21: 5293–5317.
- Sung C-H and Abrahamson NA (2022) A partially nonergodic ground-motion model for Cascadia interface earthquakes. *Bulletin of the Seismological Society of America* 112: 2520–2541.
- Tiwari A, de la Torre C, Bradley B, Lee R and Kuncar F (2023) Trends in systematic site residuals with geomorphic categories for New Zealand ground-motion instrument sites. In: *2023 New Zealand Society of Earthquake Engineering Conference*, Auckland, New Zealand, 19–21 April.
- Villani M and Abrahamson NA (2015) Repeatable site and path effects on the ground-motion sigma based on empirical data from Southern California and simulated waveforms from the CyberShake platform. *Bulletin of the Seismological Society of America* 105: 2681–2695.
- Wotherspoon LM, Kaiser AE, Stolte AC and Manea E (2023) Development of the site characterisation database for the NZ NSHM. *Seismological Research Letters* 95: 214–225.